

Modulating Lysosomal pH through Innovative Multimerized Succinic Acid-Based Nucleolipid Derivatives

Mathias Brouillard, Rémi Kinet, Marie Joyeux, Benjamin Dehay,* Sylvie Crauste-Manciet, and Valérie Desvergnès*



Cite This: <https://doi.org/10.1021/acs.bioconjchem.3c00041>



Read Online

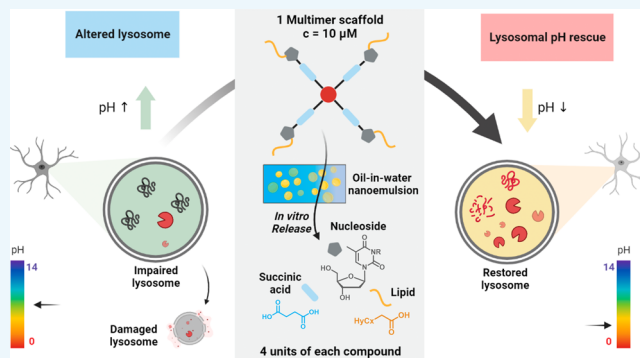
ACCESS |

Metrics & More

Article Recommendations

Supporting Information

ABSTRACT: The multimerization of active compounds has emerged as a successful approach, mainly to address the multivalency of numerous biological targets. Regarding the pharmaceutical prospect, carrying several active ingredient units on the same synthetic scaffold was a practical approach to enhance drug delivery or biological activity with a lower global concentration. Various examples have highlighted better *in vivo* stability and therapeutic efficiency through sustained action over monomeric molecules. The synthesis strategy aims to covalently connect biologically active monomers to a central core using simple and efficient reaction steps. Despite extensive studies reporting carbohydrate or even peptide multimerization developed for therapeutic activities, very few are concerned with nucleic acid derivatives. In the context of our efforts to build non-viral nucleolipid (NL)-based nanocarriers to restore lysosomal acidification defects, we report here a straightforward synthesis of tetrameric NLs, designed as prodrugs that are able to release no more than one but four biocompatible succinic acid units. The use of oil-in-water nanoemulsion-type vehicles allowed the development of lipid nanosystems crossing the membranes of human neuroblastoma cells. Biological evaluations have proved the effective release of the acid within the lysosome of a genetic and cellular model of Parkinson's disease through the recovery of an optimal lysosomal pH associated with a remarkably fourfold lower concentration of active ingredients than with the corresponding monomers. Overall, these results suggest the feasibility, the therapeutic opportunity, and the better tolerance of multimeric compounds compared to only monomer molecules.



INTRODUCTION

Although the underlying mechanisms leading to neurodegenerative diseases, including Alzheimer's and Parkinson's diseases, remain uncertain, one of the common pathological hallmarks is the loss of lysosomal degradation efficiency. Some aspects of this feature include an impaired hydrolytic pH-dependent activity,¹ leading to a defective maturation process of the lysosomal proteases in the luminal compartment,^{2,3} which in turn induces the subsequent accumulation of non-degraded aggregation-prone proteins as significant factors of neurodegeneration.⁴ Thus, therapeutic approaches targeting lysosomes to favor an impaired pH decrease have been proven to be a promising strategy in animal models.^{5,6} Nevertheless, there was a lack of systems to achieve lysosomal acidification in therapeutics. Some acid-based molecules have shown interesting properties; in particular, poly(DL-lactide-co-glycolide) (PLGA) has been described as an efficient acidifying active ingredient⁷ that releases two monomers: lactic acid and glycolic acid.⁸ Different nanosystems were developed to facilitate PLGA crossing of biological membranes, such as acidic nanoparticles (NPs)^{5,6} and acidic oil-in-water (O/W)

nanoemulsions (NEs),⁹ to cross the blood–brain barrier.¹⁰ However, PLGA polymer formulation presents some loading limitations. To overcome the shortcomings of the current chemical arsenal, we have recently developed the first low-molecular-weight acid-based nucleolipid (NL) nanocarriers carrying the biocompatible organic succinic diacid to the lysosome as a potential lysosomal acidifying agent, thanks to its excellent biocompatibility and its pKa range remarkably close to lactic and glycolic acids pKas.¹¹ This result paved the way for the development of such NL-based compounds. We have considered a multimerization-based approach to both decrease the prodrug concentration and overcome the cytotoxicity observed for some of our NL compounds. Multimeric compounds are much less explored but are nonetheless

Received: January 30, 2023

Revised: January 31, 2023

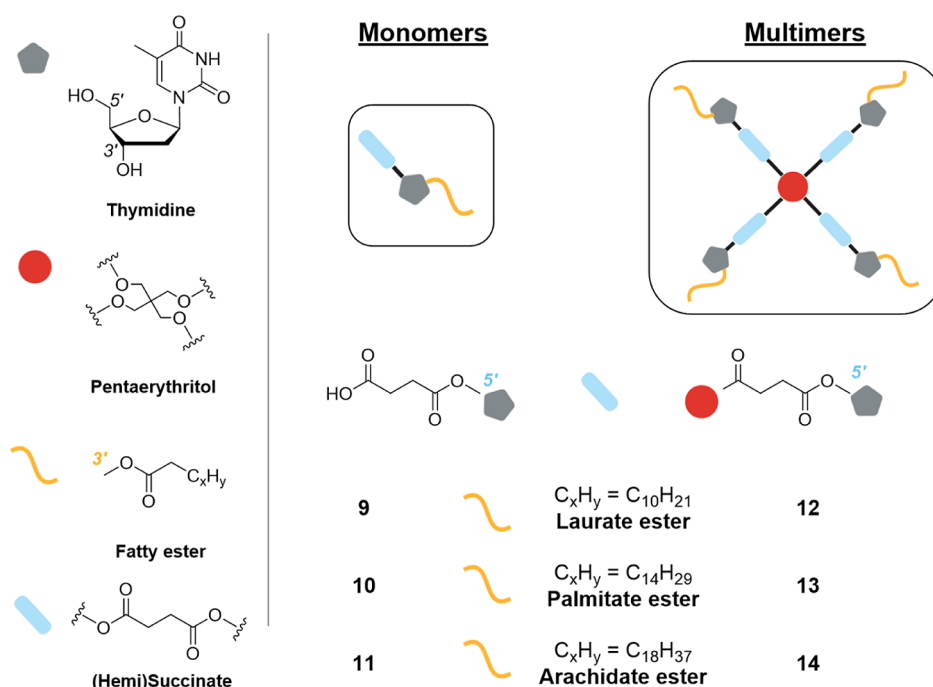


Figure 1. Schematic illustration of the monomeric and multimeric series. Compounds 9, 10, and 11 are monomeric NLs with laurate ester, palmitate ester, and arachidate ester as fatty chain at 3' position, respectively. Compounds 12, 13, and 14 are the multimers NLs with laurate ester, palmitate ester, and arachidate ester at 3' position, respectively.

promising alternatives for neurodegenerative diseases.¹² To our knowledge, only one synthetic multimeric compound was reported to modulate lysosome inner core pH.¹³ Multimeric compounds consist of several monomeric molecules tethered together owing to a single backbone. This modification was inspired by multimeric structures of proteins and is primarily illustrated by dendrimers. These compounds are synthetic and complex macromolecular multimers chemically mainly designed to provide multivalent ligands to receptors^{14,15} but not only. Regarding future therapeutic developments, multimerization appeared to be an effective strategy to enhance drug delivery or biological activity with a lower global concentration.¹² Various examples have highlighted better *in vivo* stability¹⁶ and therapeutic efficiency through a sustained action¹⁷ over monomeric molecules. This approach has been successfully used to optimize the biological efficiency of peptides,¹⁶ nucleic acids,¹⁷ or therapeutic antibodies,¹⁸ but no examples are reported concerning simple nucleoside derivatives. If dendrimers have recently been the subject of much interest in medicine, serious challenges remain for their design, large-scale synthesis, characterization, and formulation.¹⁵ To overcome these drawbacks and keep structural flexibility and size, allowing the incorporation of NEs, we decided to synthesize simpler compounds, which could be seen as low-generation dendrimers.

We describe herein the conception and the synthesis of the first series of multimeric thymidine-based prodrugs carrying four effective biocompatible organic acid units as a therapeutic ingredient (Figure 1).

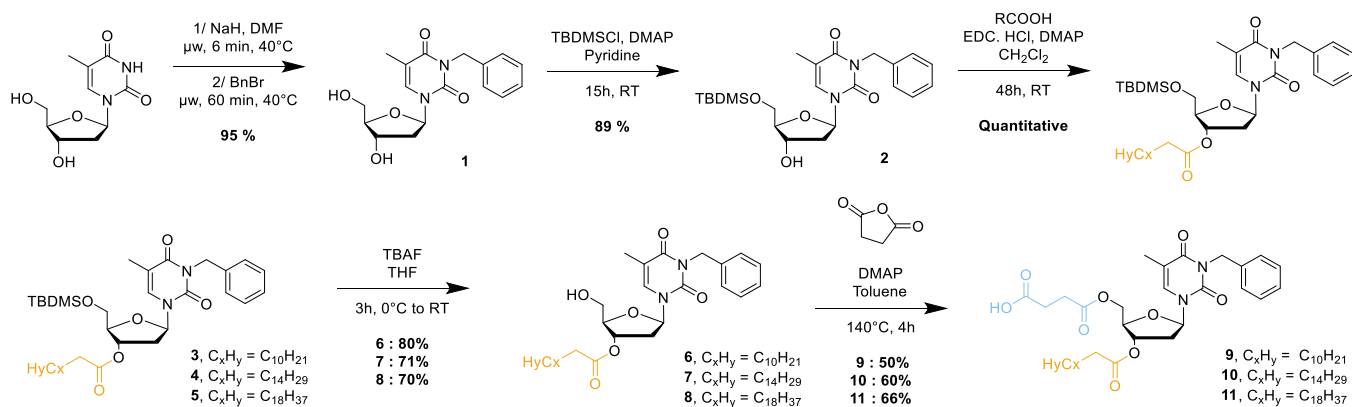
A convergent and straightforward synthesis was achieved based on esterification steps to allow cleavable links under the enzymatic stimulus. Indeed, the protection of the succinic acid as succinate moieties at the inner position of the edifice was then supposed to be a real asset for a sustained release of the active ingredient under lysosomal esterase action. Lipophilicity

and size of the compounds were modulated with the nature of the fatty chain at the 3' position on the nucleoside. As for the monomer analogues, the prodrugs were encapsulated within O/W NE vehicles, performing a system to overcome barriers,¹⁹ including the blood–brain barrier. The cellular viability was evaluated on human neuroblastoma cell lines. Then, biological assays on a genetic and cellular model of Parkinson's disease were performed to investigate their acidifying potential rescue. These results confirm the therapeutic potential of these new NL-based nanosystems and highlight lysosomal restoration as a disease-modifying strategy for treating Parkinson's disease and other age-related proteinopathies. In particular, these results hold out the hope of modulating drug release by varying the nature of the fatty chain, which would be of great interest in chronic treatment with sustained release.

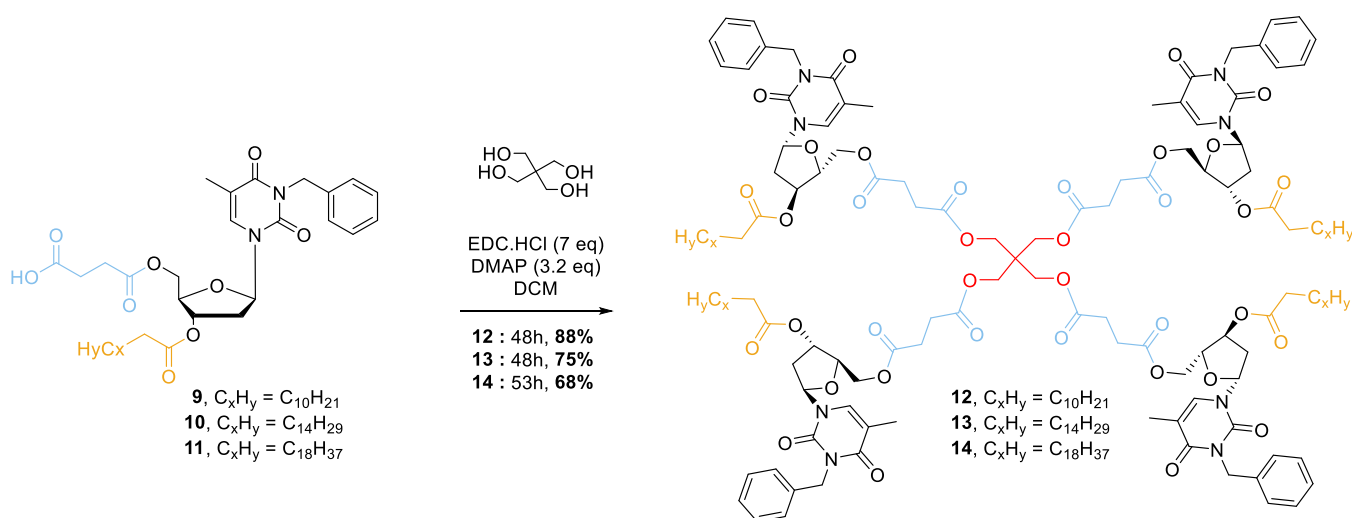
RESULTS AND DISCUSSION

Conception and Synthesis of the Multimeric Acidic NLs. We previously reported the conception and synthesis of original NLs carrying a biocompatible succinic acid as the active ingredient. These DNA-based prodrugs were incorporated into O/W NEs and successfully crossed neuronal plasmatic membranes to acidify lysosomal pH.¹¹ Original compounds bearing two different monocatenar fatty chains as esters groups at the 3'-position (palmitate and arachidate) were then synthesized. Palmitate compound 10, first designed based on preliminary results,²⁰ was shown to induce acute cell toxicity at 24 h of exposure for the NE loaded with 3% w/w, whereas arachidate compound 11 induced no cytotoxicity even at a higher 7% w/w concentration. As the lysosomes play a central role in lipid transport, catabolism, and biogenesis, the cytotoxicity of compound 10 toward M17 neuronal cell lines could be related to the release of palmitate inside the lysosome. Indeed, the lipotoxicity of palmitate²¹ has been previously reported to be associated with a lumen alkalization, a

Scheme 1. Synthetic Pathway to Generate Monomeric NL 9–11



Scheme 2. From Monomers to Multimers: Steglich Reaction-Based One-Step Efficient Access



suppression of hydrolase activity, and an impairment of lysosomal function, particularly in pancreatic β -cells.²² To investigate the influence of the fatty chain length onto the cell tolerance, the laurate derivative **9** was also synthesized following the same synthetic optimized pathway as previously reported for compounds **10** and **11** (Scheme 1).

Multimerization was reported as an attractive approach to ensure higher stability in the case of RNA therapeutics.¹⁷ Tetra-branched analogues of bioactive neuropeptides exhibited better stability to protease activity and a higher half-life than their monomeric counterparts.²³ Such an approach for our NL-based acidifying compounds was planned to synthesize a tetrameric scaffold to hinder the chemical structure. Moreover, tuning the surface functionality with the incorporation of the NL skeleton on the outer surface and the insertion of the succinic acid units as succinate at the inner core of the molecule was of interest to modulate the hydrophilic/lipophilic properties of this molecule. It was expected to provide convenient lipophilicity to the molecule for its further incorporation into O/W NEs and to subsequently achieve a passive cellular uptake. Thus, three original tetrameric acidic NLs carrying masked succinic acids derived from the monomeric compounds were targeted following a straightforward synthetic pathway. Previous unpublished work highlighted the low reactivity at the 5' position when the 3' position was hindered with a fatty chain. With the hemi-

succinate as spacer, NL derivatives **9**, **10**, and **11** were then used to successfully implement an efficient classical Steglich-type esterification key step with pentaerythritol, providing the desired tetrameric compounds **12**, **13**, and **14** in good yields (Scheme 2). NLs **12**, **13**, and **14** were thus prepared *via* a seven-step sequence from natural thymidine, respectively, in 30, 27, and 26% satisfactory overall yields. The compound **12** bearing a laurate ester at a 3' position was obtained in a slightly better overall yield than its C16 and C20 ester analogues, certainly for steric reasons.

Formulation and Physical Characteristics of O/W NEs.

Despite many efforts, one of the main issues for developing new therapeutics targeting the central nervous system (CNS) diseases is the difficult crossing of the poorly permeable blood–brain barrier that retains more than 98% of molecules, including drugs.²⁴ Among the promising nanocarrier systems²⁵ for improving CNS neuropharmacokinetics, NEs have a prominent place.^{10,26} These colloidal dispersions of two non-miscible phases (O/W) are particularly suitable for carrying and delivering lipophilic drugs. Moreover, such systems display droplets on the nanometric scale, making them appropriate for administration through several routes, including systemic injection. The surface/volume ratio provides a high loading rate, and the colloidal stability of the system justifies an actual use in clinics. Furthermore, these formulations allow protection from premature enzymatic or chemical degrada-

Table 1. Physicochemical Characteristics of Monomeric and Multimeric NL NEs

	control		lauric acid series		palmitic acid series		arachidic acid series	
	NE-0	NE-9	NE-12	NE-10	NE-13	NE-11	NE-14	
droplet mean diameter (nm)	164.1 ± 1.3	159.9 ± 4.7	193.6 ± 5.0	170.6 ± 2.0	179.3 ± 3.4	194.0 ± 3.1	171.9 ± 1.7	
polydispersity index	0.094	0.096	0.126	0.077	0.099	0.113	0.112	
ζ potential (mV)	-33.6 ± 0.2	-30.8 ± 0.2	-36.8 ± 0.8	-39.1 ± 1.8	-30.2 ± 0.4	-37.0 ± 0.7	-33.6 ± 0.2	
pH	5.9	3.7	5.3	4.2	5.1	3.9	5.6	

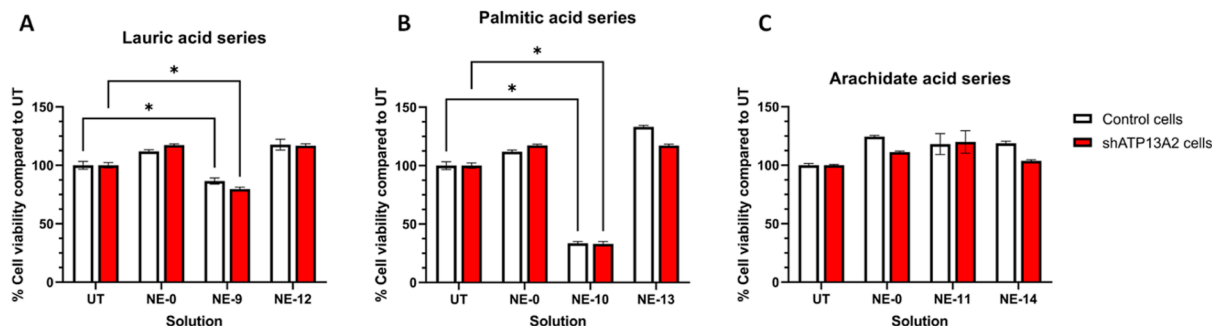


Figure 2. Comparative cell viability in control and ATP13A2-depleted (shATP13A2) M17 cells in the absence (UT) or presence of NE for each fatty chain length 24 h after treatment. * $p < 0.05$ compared with untreated cells. (A) NE-0, NE-9, and NE-12. (B) NE-0, NE-10, and NE-13. (C) NE-0, NE-11, and NE-14.

tion.²⁷ All O/W NEs were produced with 20% medium-chain triglyceride oil (Miglyol 812N) and 1.2% lecithin 80 and 2.5% polysorbate 80 as surfactants. Surfactants were added to permit the emulsification and stabilize the dispersion over time. The 80% aqueous phase also contains glycerol to adjust the tonicity. Similarly to our previous work, monomeric compound 9 was solubilized at 3% (w/w) in the oily phase. To release theoretically the same quantity of acid units, tetramers 12, 13, and 14 were loaded at a molar concentration equivalent to a quarter of the monomers' one (10 μ M). NE-9, NE-10, and NE-11 were loaded with acidic NLs 9, 10, and 11, respectively. Tetramers 12, 13, and 14 were successfully solubilized in oil and loaded with final concentrations at 3% (w/w) to provide the subsequent NE-12, NE-13, and NE-14, respectively. All these formulations exhibited similar granulometric profiles with NE loaded with monomer counterparts and the unloaded NE-0 used as a control. The average diameter measured by dynamic light scattering (<200 nm) displayed a compatible size for cellular uptake and negative ζ potential favoring less toxicity than positively charged nano-objects (Table 1). The physicochemical characteristics of NE-12, NE-13, and NE-14, loaded with tetramer compounds, did not exhibit any significant change for at least 3 months.

To ensure our synthetic compound integrity inside the NEs and the cleavage of ester bonds to release succinic acid from succinate derivatives, an acid–base titration of NE was performed using NaOH solution (0.5 M), and the pH was monitored. The experiments were carried out on unloaded control NE-0, an NE loaded with the monomeric arachidate NL 11, and a nanoemulsion loaded with tetrameric arachidate NL 14. The three curves exhibited clearly different shape profiles (Figure S1). The profile of the NE-11 curve is fully consistent with a weak diacid titration. In contrast, the titration curve of NE-14 showed eight successive pH increases, which is rational with the expected subsequent release of four succinic acid units.

Assessment of the Cellular Viability of the Different Loaded NEs. Before the evaluation of the acidifying efficacy of

our compounds, *in vitro* viability assays were performed on control cells and on a cellular model displaying abnormally high pH in their lysosomes (shATP13A2)^{7,28–31} (Figure 2). The results showed that NE-12 (Figure 2A), NE-13 (Figure 2B), and NE-14 (Figure 2C), respectively, loaded with 3% (w/w) 12, 13, and 14, did not induce cell death after 24 h exposure compared to NE-9 (Figure 2A) and NE-10 (Figure 2B), highlighting an impressive effect of the tetramers compared to monomers. Although nothing related to this was reported in the literature, to our knowledge, it is noticeable that laurate compound 9 was as cytotoxic as its palmitate analogue. Outstandingly, NE-12, NE-13, and NE-14, regardless of the 3'-fatty chain, did not induce cell death up to 72 h exposure (Figures S2 and S3).

Complementary cytotoxicity studies were performed to evaluate nucleus integrity (Figure 3A) and detect DNA strand breaks (Figure 3B) after treatment with NE loaded with 3% (w/w) of the cytotoxic monomer compound 9 and NE-12, NE-13, and NE-14, respectively, loaded with tetramers 12, 13, and 14. These additional results confirmed that the tetrameric compounds did not induce any significant cytotoxicity.

Further investigations advertised the absence of cytotoxicity of single NLs 6, 7, and 8 compounds, both synthetic intermediates and products of the prodrug degradative pathway after 24 h (Figure 4) and 48–72 h (Figure S4) of treatment. These results strengthen the choice of tetrameric compounds as biodegradable and biocompatible prodrugs.

Lysosomal pH Measurement. ATP13A2-depleted M17 cells were used to evaluate the acidification potential of the NEs onto sick lysosomes. Indeed, the depletion of ATP13A2 induces an abnormally high lysosomal pH.^{7,28–31} First, in this proof-of-concept study, we have chosen a time point of 24 h of treatment to be under the ideal and controlled condition to reveal the potential of these new molecules in relation to lysosomal dysfunction and therapeutic approaches. A time point of 24 h is a controlled processing time of treatment where we can reveal the lysosomal impairment and appreciate the possible acidification effect on these shATP13A2 cells with

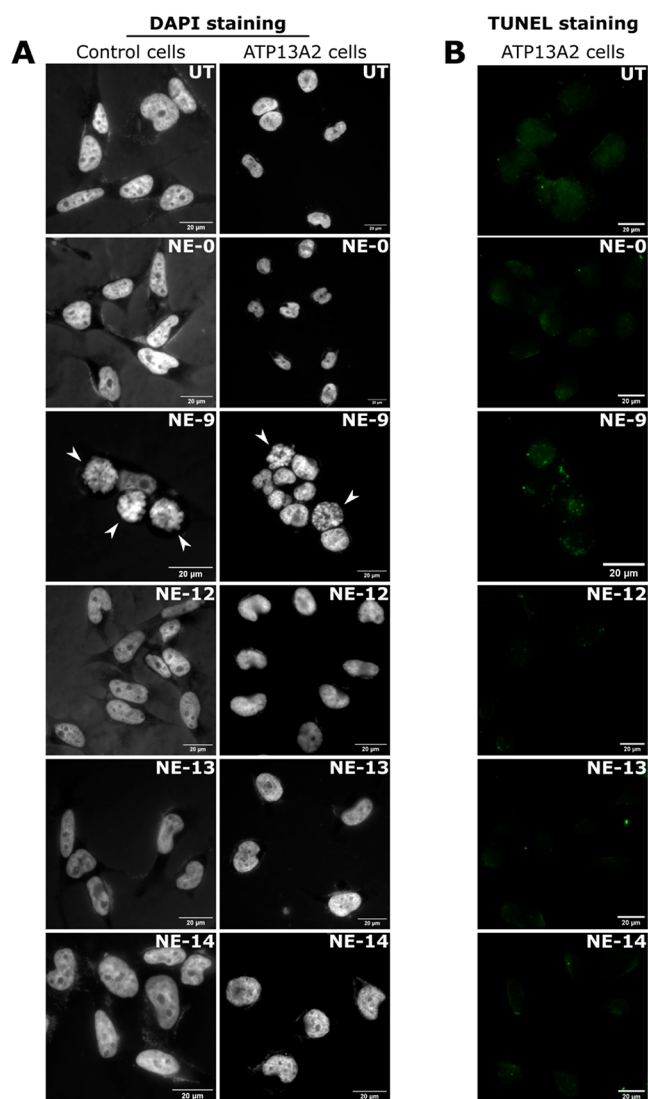


Figure 3. Illustration of the cellular and nuclear morphology in control and ATP13A2-depleted (ATP13A2) M17 cells in the absence (UT) or presence of NE-0, NE-9, NE-12, NE-13, and NE-14 24 h after treatment. (A) DAPI staining in control and ATP13A2-depleted cells, treated during 24 h with NE-0, NE-9, NE-12, NE-13, and NE-14. Arrowheads show apoptotic nucleus forms, present under the NE-9 condition. (B) TUNEL staining in ATP13A2-depleted cells, treated during 24 h with NE-0, NE-9, NE-12, NE-13, and NE-14. TUNEL assay should show a green dot if degraded DNA within a nucleus is detected, as this assay is based on detecting single- and double-stranded DNA breaks that occur at the early stages of apoptosis. Puncta show free 3'-OH groups in single- and double-stranded DNA. The NE-9 condition shows multiple puncta compared to other conditions.

a panel of acidic compounds.^{5,6,9,11} *In vitro* lysosomal pH measurements of NL-based NEs, loaded at 3% (w/w), were carried on by comparing tetramer-loaded NEs and the NE loaded with the corresponding succinate NL monomer. In the case of 9 and 10 bearing, respectively, a laurate and a palmitate chain at 3' position, no evaluation could be performed due to their toxicity (Figure 2A,B). Remarkably, the NE derived from their tetramer counterparts NE-12 and NE-13 were found to decrease lysosomal pH of 1.3 and 2.4 units, respectively (Figure 5). Multimer 13 even provided a complete restoration of the lysosomal pH. Concerning the arachidate series, NE-14

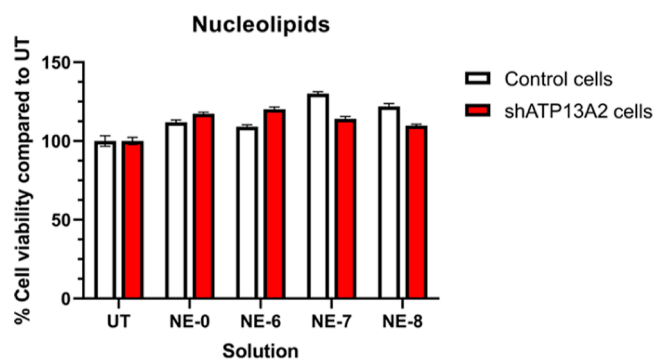


Figure 4. Cell viability in control and ATP13A2-depleted (shATP13A2) M17 cells in the absence (UT) or presence of NE-0, NE-6, NE-7, and NE-8 24 h after treatment.

loaded with the tetramer NL induced less acidification than NE-11 with, respectively, 1.6 and 3.0 units of pH decrease.

Acidification of the lysosome ensures the internal disuccinate hydrolysis, and its kinetics is definitively related to steric hindrance, which is much higher for compound 14. Indeed, several studies reported the influence of the fatty chain length on cell hydrolysis kinetics.³² A lower decrease in lysosomal pH for NE-14 compared to NE-13 is not surprising. Modulating the length of the fatty ester makes it possible to tune the acidification of the organelle medium (Table 2). Similarly, the difference between NE-14 and NE-11 could be attributed to a slower degradation of the tetrameric compound 14 which does not carry a directly accessible acid function, unlike compound 11. This promising result anticipates a sustained release of the active ingredient over time.

To go further and prove that acidification was due to succinic acid release, NEs loaded with NLs 6, 7, and 8 (Table S1) derived from the tetramer degradation were submitted to the same experiments of lysosomal pH measurement (Figure S5). No significant acidification was measured, suggesting that a potential cleavage of fatty esters at the 3' position and subsequent release of the corresponding fatty acids do not promote any acidification either. Taken together, these results revealed the relevance of multimerizing therapeutic prodrugs to emphasize their efficiency.

CONCLUSIONS

Restoring an acidic pH in the lysosome appeared to be a promising approach to preserve the autophagic process and, in turn, cellular homeostasis. Thus, the repair of lysosomal pH has been the subject of increasing interest for several years, despite the few chemical agents to target this organelle. Previous results reported the significant benefit of using known biocompatible acidic NL-based nanocarriers to rescue lysosomal impairment in a disease cellular model. To enhance NL-based prodrug stability and lower the global concentration from a pharmaceutical perspective, NL multimerization emerged as a chemical modification of interest. In this study, emphasis was given to the use of simple and robust chemical steps to achieve a straightforward synthesis from thymidine. Multimeric compounds 12, 13, and 14 were designed as prodrugs by analogy with monomeric acidic NLs 9, 10, and 11, carrying the same fatty chains and biocompatible succinic acid. For solubility reasons, succinic acid was "masked", and succinate moieties were placed at the inner part of the molecule. The compounds were then successfully solubilized

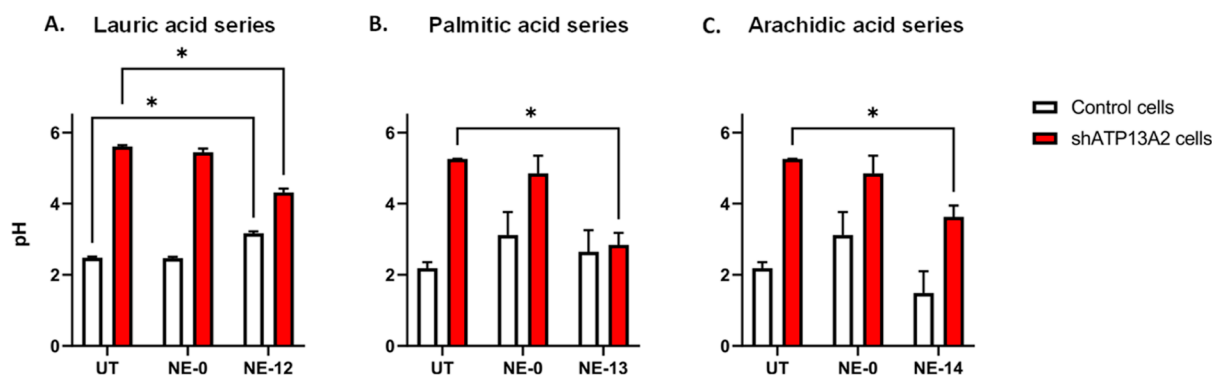


Figure 5. Lysosomal pH *in vitro* in control and ATP13A2-depleted (shATP13A2) M17 cells, in the absence (UT) or presence of NE-0 and multimeric NEs NE-12, NE-13, and NE-14. *, $p < 0.05$ compared with shATP13A2 untreated cells.

Table 2. NL-Based NE Restores Lysosomal pH *In Vitro* 24 h After Treatment

compound	lauric acid series		palmitic acid series		arachidic acid series	
	9	12	10	13	11	14
Δ pH (u. pH)	n.d.	-1.3 ^a	n.d.	-2.4 ^a	-3.0 ^a	-1.6 ^a

^aLysosomal pH values in ATP13A2-depleted (shATP13A2) M17 cells. * $p < 0.05$ compared with shATP13A2 untreated cells. n.d.: not determined. Assay cannot be performed due to the cytotoxicity of the compound.

into O/W NE oily phases to cross biological membranes. In contrast to monomers **9** and **10**, no tetramer-derived NE (**10** μ M) exhibited significant toxicity (up to 72 h) on genetic model cell lines of Parkinson's disease. Noticeably, NE-13, loaded with palmitate tetramer derivative **13**, ultimately rescued the lysosomal pH 24 h after treatment. Drug release from NL tetramers **12**, **13**, and **14** depends on the chemical structure and may be controlled by tunable properties related to stability, solubility, and biodegradation. Indeed, modulating their surface and, consequently, their size and lipophilicity with various fatty chain lengths could allow adjustment of such physicochemical properties for further formulation optimization.

To date, these NLs are the most effective non-polymeric acidifying compounds to address lysosomal pH impairment. The reliable synthesis of these molecules is easily reproducible on a larger scale, and the efficient encapsulation in NE O/W ensures optimized stability, homogeneity, and drug loading. To optimize the potential of these innovative nanosystems, further *in vivo* evaluations will be performed to evaluate their ability to cross the blood–brain barrier after systemic administration.

EXPERIMENTAL SECTION

¹H NMR and ¹³C NMR were recorded at 293 K on a Bruker Avance 300 (¹H: 300 MHz, ¹³C: 75.46 MHz) spectrometer using residual CHCl₃ as an internal reference (7.26 ppm). The chemical shifts (δ) and coupling constants (J) are expressed in ppm and Hz. The following abbreviations were used to explain the multiplicities: s = singlet, d = doublet, t = triplet, and m = multiplet. Fourier transform infrared (FT-IR) spectra were recorded on a PerkinElmer FT spectrometer Spectrum two (UATR two). For electrospray ionization (ESI) high-resolution mass spectrometry (HRMS) analyses, a Waters Micromass ZQ instrument equipped with an electrospray source was used in the positive and/or negative mode. Matrix-

assisted laser desorption ionization time-of-flight (MALDI-TOF) mass spectrometric analyses were performed on a PerSeptive Biosystems Voyager-De Pro MALDI mass spectrometer in the linear mode using 3,4-dihydroxybenzoic acid as the matrix. Analytical thin-layer chromatography was performed using silica gel 60 F254 precoated plates (Merck) with visualization by ultraviolet light, potassium permanganate, or sulfuric acid. Flash chromatography was performed on a silica gel (0.043–0.063 mm).

Synthesis and Characterization of Multimeric Succinic Acid-Based NLs. *General Procedure of Succinic Acid-Based NL Synthesis.* To a solution of monomeric acidic NL compounds (10 equiv) in dry DCM (0.1 g mL⁻¹) was added under argon pentaerythritol (1 equiv), EDC HCl (7 equiv), and DMAP (3.2 equiv). The reaction mixture was stirred at room temperature for 48 h under an argon atmosphere. The crude product was purified by flash chromatography over silica gel (toluene/acetone: 80/20 + Et₃N 0.1%) to provide multimeric compounds **12**, **13**, and **14** as colorless gums.

Compound 12. $R_f = 0.4$ (toluene/acetone: 80/20 + NEt₃); IR (ATR) ν_{\max} (cm⁻¹) 2925, 2855, 1742, 1706, 1671, 1465, 1257, 1157, 767, 701;

¹H NMR (300 MHz, CDCl₃) δ (ppm) 7.49–7.21 (m, 6H), 6.36 (dd, $J = 5.4, 8.7$ Hz, 1H), 5.23–5.12 (m, 1H), 5.12 (s, 2H), 4.37 (ddd, $J = 4.5, 12, 16.5$ Hz, 2H), 4.24–4.18 (m, 1H), 4.16–4.09 (m, 4H), 2.71–2.58 (m, 4H), 2.45 (dd, $J = 5.7, 14.1$ Hz, 1H), 2.33 (appearing t, $J = 7.2, 7.8$ Hz, 2H), 2.23–2.10 (m, 1H), 1.96 (s, 3H), 1.70–1.54 (m, 2H), 1.41–1.17 (m, 32H), 0.95–0.83 (m, 3H); ¹³C NMR (75.5 MHz, CDCl₃) δ (ppm) 173.3, 171.8, 163.2, 151.0, 136.9, 132.9, 129.2, 128.5, 127.7, 110.9, 85.6, 82.2, 74.1, 64.3, 62.5, 44.7, 37.5, 34.2, 32.0, 29.7, 29.5, 29.4, 29.3, 29.2, 28.8, 28.7, 24.9, 22.8, 14.2, 13.5; HRMS (ESI): calcd for C₁₃₇H₁₈₈N₈O₃₆ [M/2+2H]²⁺, 1262.67196; found, 1262.66631.

Compound 13. $R_f = 0.4$ (toluene/acetone: 80/20 + NEt₃); IR (ATR) ν_{\max} (cm⁻¹) 2926, 2855, 1739, 1704, 1669, 1645, 1266, 1152, 734, 701, 537;

¹H NMR (300 MHz, CDCl₃) δ (ppm) 7.52–7.23 (m, 6H), 6.36 (dd, $J = 5.7, 8.7$ Hz, 1H), 5.25–5.18 (m, 1H), 5.12 (s, 2H), 4.38 (ddd, $J = 4.2, 12, 16.5$ Hz, 2H), 4.25–4.18 (m, 1H), 4.17–4.08 (m, 4H), 2.73–2.60 (m, 4H), 2.46 (dd, $J = 5.4, 13.5$ Hz, 1H), 2.33 (appearing t, $J = 7.5, 7.8$ Hz, 2H), 2.25–2.10 (m, 1H), 1.97 (s, 3H), 1.69–1.55 (m, 2H), 1.41–1.18 (m, 24H), 0.90 (t, $J = 6.7$ Hz, 3H); ¹³C NMR (75.5 MHz, CDCl₃) δ (ppm) 173.3, 171.8, 163.2, 151.0, 136.9, 132.9, 129.2, 128.5, 127.7, 110.8, 85.6, 82.2, 74.1, 64.3, 62.5, 44.7, 37.5, 34.2, 32.0, 29.8, 29.7, 29.7, 29.6, 29.5, 29.3, 29.2, 28.8, 28.7, 24.9, 22.8,

14.2, 13.5; HRMS (ESI): calcd for $C_{153}H_{220}N_8O_{36}$ $[M/2+2H]^{2+}$, 1374.78152; found, 1374.29217.

Compound 14. $R_f = 0.5$ (toluene/acetone: 85/15);

IR (ATR) ν_{max} (cm⁻¹) 2925, 2854, 1740, 1704, 1670, 1466, 1272, 1156, 766, 700;

¹H NMR (300 MHz, CDCl₃) δ (ppm) 7.52–7.22 (m, 6H), 6.36 (dd, $J = 5.4, 8.7$ Hz, 1H), 5.25–5.17 ppm (m, 1H), 5.13 (s, 2H), 4.38 (ddd, $J = 4.5, 12, 16.5$ Hz, 2H), 4.24–4.18 (m, 1H), 4.17–4.09 (m, 4H), 2.60–2.51 (m, 4H), 2.45 (dd, $J = 6.0, 12.9$ Hz, 1H), 2.33 (appearing t, $J = 7.2, 7.8$ Hz, 2H), 2.23–2.10 (m, 1H), 1.96 (s, 3H), 1.70–1.55 (m, 2H), 1.39–1.19 (m, 32H), 0.95–0.85 (m, 3H); ¹³C NMR (75.5 MHz, CDCl₃) δ (ppm) 173.3, 171.8, 163.3, 151.1, 136.9, 132.9, 129.3, 128.5, 127.8, 110.9, 85.6, 82.0, 74.1, 64.3, 62.6, 44.7, 37.6, 34.3, 32.0, 29.7, 29.5, 29.4, 29.3, 28.7, 24.8, 22.8, 14.2, 13.5; HRMS (ESI): calcd for $C_{169}H_{252}N_8O_{36}$ $[M/2+2H]^{2+}$, 1486.90672; found, 1486.41702.

NE Formulation and Characterization. NE Preparation.

For biological evaluations, all O/W NEs were used as freshly prepared. The oily phase was composed of the dispersion of 12 mg of egg lecithin (Lipoid E80) into 200 mg of 70 °C heated medium-chain triglyceride oil (Miglyol 812N). To obtain the aqueous phase, 25 mg of Polysorbate 80 (Tween 80) was dispersed in 800 mg of 70 °C heated Milli-Q water. Glycerol at 2.25% was added to the aqueous phase to adjust osmolality for *in cellulo* experiments. All NL compounds were solubilized into the oily phase, at various NE final concentrations.

Phase inversion, with prepared heated phases and sonication (Sonic Vibra Cell-VC 250), provided the emulsions with nanometric size range oil droplets. NE composition in % w/w is specified in Table 3.

Table 3. NL-Based NE Typical Composition

	NE-NL (%)
NL (%) w/w	3
Lipoid E80	1.2
Miglyol 812N	20
Tween 80	2.5
glycerol	2.25
H ₂ O qs	100

NE Characterization. Droplet mean diameter and granulometric profiles of these NL-loaded NEs were evaluated using a dynamic light scattering device from Malvern Instruments (Zetasizer Nano ZS). Hydrodynamic mean diameters were assessed by three independent measurements, at 25 °C, on 1/2500 (v/v) diluted NE. ζ potential measurements were achieved on diluted NE using Zetasizer Nano ZS coupled with Folded Capillary Cell (DTS1060) from Malvern Instruments.

Cell Culture and Cell Viability Assay. Human neuroblastoma cell lines BE(2)-M17 were obtained from ATCC (CRL-2267)³³ and grown in OPTIMEM (Life Technologies, 31985-047) and 10% fetal bovine serum (Sigma-Aldrich). Impaired human dopaminergic neuroblastoma cells were obtained from ATP13A2 stable knockdown BE(2)-M17 (shATP13A2(403-1)). Cells were maintained at 37 °C in 5% CO₂ in OPTIMEM supplemented with 10% fetal calf serum, 1% penicillin/streptomycin, and 2 mg/mL puromycin (Sigma-Aldrich). For NE evaluations, cells grown at 70% to 80% confluence were treated with 1 μ L of NL-based NE diluted to 1/1000. Each experiment was reproduced at least in three

independent series. MTT assay (ATCC/LGC Promochem) provided cell viability rate, following manufacturer instructions.

Control and shATP13A2 cells were plated on coverslips in a six-well plate to evaluate the nucleus integrity. Cells were maintained for 24 h at 37 °C in 5% CO₂ before being treated with the different NEs. Cell coverslips were fixed at 4 °C for 20 min using 4% paraformaldehyde. Coverslips were finally stained with DAPI solution (Invitrogen) at 10 μ M for 8 min before long washes in PBS1X and mounted onto slides using a mounting solution (Dako). Image acquisitions were made on a wide-field Olympus epifluorescence Microscope (BX3-CBH) coupled with a Hamamatsu camera (ORCA-Flash 4.0 LT). The In Situ Cell Death Detection Kit (TUNEL Assay, Roche Cat. no. 11 684 817 910) was applied to detect DNA strand breaks in the cells at a single cell level following the manufacturer's instructions. Briefly, cell coverslips were blocked with 3% H₂O₂ in methanol for 10 min at RT, followed by washes in PBS. The slides were then permeabilized with 0.1% Triton X-100 in 0.1% sodium-citrate PBS for 2 min and rinsed twice in PBS. Then, the TUNEL reaction mixture was added to the slides. The slides were incubated in a humidified chamber in the dark at 37 °C for 1 h, then washed three times in PBS, and mounted onto slides using a mounting solution (Dako). The stained coverslips were observed under a wide-field Olympus epifluorescence microscope (BX3-CBH) coupled with a Hamamatsu camera (ORCA-Flash 4.0 LT).

Lysosomal pH Measurement. Lysosomal pH was determined using dextran conjugate LysoSensor Yellow/Blue DND-160 (Life Technologies) and was performed as previously described.^{7,34} Control and mutant ATP13A2 cells were grown in their respective media before being trypsinized, harvested (1×10^6 cells/mL), and loaded with 1 mg/mL LysoSensor dextran for 1 h at 37 °C with 5% CO₂. Then, the cells were washed three times in HBSS (Gibco, 14060) and aliquoted at 100 mL into a black 96-well microplate. All cells were treated with 10 mM monensin and 10 mM nigericin (Sigma-Aldrich) in MES buffer (5 mM NaCl, 115 mM KCl, 1.3 mM MgSO₄, and 25 mM MES), with the pH adjusted to a range from 3.5 to 7.0. The samples were read in a FLUOstar Optima fluorimeter (BMG Labtech, Champigny Sur Marne, France) with excitation at 355 nm. The emission 440/535 nm ratio was then calculated for each sample. The pH values were determined from the standard linear curve generated *via* the pH calibration performed as previously described.

Statistical Analysis. Statistical analysis was performed in GraphPad Prism 6 software. NE density quantification was analyzed by unpaired *t*-test. For functional assays, the statistical significance of the data was evaluated after the calculation of a one-way or two-way analysis of variance (ANOVA) followed by Tukey's multiple comparison test. The level of significance was set at $p < 0.05$. All data are expressed as mean \pm SEM unless indicated otherwise.

■ ASSOCIATED CONTENT

SI Supporting Information

The Supporting Information is available free of charge at <https://pubs.acs.org/doi/10.1021/acs.bioconjchem.3c00041>.

Compounds 3, 6, and 9 synthetic experimental procedures, all ¹H and ¹³C NMR spectra, 5'-OH NL NE characterization, and cell viability assays for monomer NLs 48 h after treatment, for multimer NLs, and 5'-OH NLs at 48 h and 72 h (PDF)

AUTHOR INFORMATION

Corresponding Authors

Benjamin Dehay – Univ. de Bordeaux, CNRS, IMN, UMR 5293, Bordeaux F-33000, France; orcid.org/0000-0003-1723-9045; Email: benjamin.dehay@u-bordeaux.fr

Valérie Desvergnès – University of Bordeaux, INSERM U1212, UMR CNRS 5320, Bordeaux 33405, France; orcid.org/0000-0003-0290-8875;

Email: valerie.desvergnès@u-bordeaux.fr

Authors

Mathias Brouillard – University of Bordeaux, INSERM U1212, UMR CNRS 5320, Bordeaux 33405, France

Rémi Kinet – Univ. de Bordeaux, CNRS, IMN, UMR 5293, Bordeaux F-33000, France; orcid.org/0000-0002-7737-6837

Marie Joyeux – University of Bordeaux, INSERM U1212, UMR CNRS 5320, Bordeaux 33405, France

Sylvie Crauste-Manciet – University of Bordeaux, INSERM U1212, UMR CNRS 5320, Bordeaux 33405, France; Univ. Angers, CHU Angers, INSERM, CNRS, MINT, SFR ICAT, F-49000 Angers, France

Complete contact information is available at:

<https://pubs.acs.org/10.1021/acs.bioconjchem.3c00041>

Author Contributions

M.B., R.K., M.J., and B.D. carried out experiments. B.D., S.C.-M., and V.D. designed the experiments. M.B., R.K., M.J., B.D., S.C.-M., and V.D. analyzed the data and wrote the manuscript. B.D., S.C.-M., and V.D. secured the funding. All authors read and approved the manuscript.

Notes

The authors declare no competing financial interest.

ACKNOWLEDGMENTS

M.B. is a recipient of an MSER fellowship (France). RK is a recipient of a Clément Fayat Foundation fellowship (France). We thank Marie-Laure Thiolat for technical assistance in cell culture. INSERM, CNRS, and the University of Bordeaux provided financial and infrastructural support. This study received financial support from the French government in the framework of the University of Bordeaux's IdEx "Investments for the Future" program/GPR BRAIN_2030. This study received financial support from the STS (Sciences and Technologies for Health) department of the University of Bordeaux.

REFERENCES

- (1) Ameis, D.; Merkel, M.; Eckerskorn, C.; Greten, H. EurPurification, characterization and molecular cloning of human hepatic lysosomal acid lipase. *J. Biochem.* **1994**, *219*, 905–914.
- (2) Kawai, A.; Uchiyama, H.; Takano, S.; Nakamura, N.; Ohkuma, S. Autophagosome-lysosome fusion depends on the pH in acidic compartments in CHO cells. *Autophagy* **2007**, *3*, 154–157.
- (3) Song, Q.; Meng, B.; Xu, H.; Mao, Z. The emerging roles of vacuolar-type ATPase-dependent Lysosomal acidification in neurodegenerative diseases. *Transl. Neurodegener.* **2020**, *9*, 17.
- (4) Arotcarena, M. L.; Teil, M.; Dehay, B. Autophagy in Synucleinopathy: The Overwhelmed and Defective Machinery. *Cells* **2019**, *8*, 565.
- (5) Bourdenx, M.; Daniel, J.; Genin, E.; Soria, F. N.; Blanchard-Desce, M.; Bezard, E.; et al. Nanoparticles Restore Lysosomal Acidification Defects: Implications for Parkinson and Other Lysosomal-Related Diseases. *Autophagy* **2016**, *12*, 472–483.
- (6) Arotcarena, M.-L.; Soria, F. N.; Cunha, A.; Doudnikoff, E.; Prévot, G.; Daniel, J.; Blanchard-Desce, M.; Barthélémy, P.; Bezard, E.; Crauste-Manciet, S.; Dehay, B. Acidic nanoparticles protect against a-synuclein-induced neurodegeneration through the restoration of lysosomal function. *Aging Cell* **2022**, *21*, No. e13584.
- (7) Cunha, A.; Gaubert, A.; Latxague, L.; Dehay, B. PLGA-Based Nanoparticles for Neuroprotective Drug Delivery in Neurodegenerative Diseases. *Pharmaceutics* **2021**, *13*, 1042.
- (8) Kaplan, J. A.; Lei, H.; Liu, R.; Padera, R.; Colson, Y. L.; Grinstaff, M. W. Imparting superhydrophobicity to biodegradable poly(lactide-co-glycolide) electrospun meshes. *Biomacromolecules* **2014**, *15*, 2548–2554.
- (9) Prévot, G.; Soria, F. N.; Thiolat, M.-L.; Daniel, J.; Verlhac, J. B.; Blanchard-Desce, M.; Bezard, E.; Barthélémy, P.; Crauste-Manciet, S.; Dehay, B. Harnessing Lysosomal pH through PLGA Nanoemulsion as a Treatment of Lysosomal-Related Neurodegenerative Diseases. *Bioconjug. Chem.* **2018**, *29*, 4083–4089.
- (10) Karami, Z.; Saghatchi Zanjani, M. R.; Hamidi, M. Nanoemulsions in CNS Drug Delivery: Recent Developments, Impacts and Challenges. *Drug Discov. Today* **2019**, *24*, 1104–1115.
- (11) Brouillard, M.; Barthélémy, P.; Dehay, B.; Crauste-Manciet, S.; Desvergnès, V. Nucleolipid Acid-Based Nanocarriers Restore Neuronal Lysosomal Acidification Defects. *Front. Chem.* **2021**, *9*, 736554.
- (12) Chafekar, S. M.; Malda, H.; Merx, M.; Meijer, E. W.; Viertel, D.; Lashuel, H. A.; Baas, F.; Scheper, W. Branched KLVFF tetramers strongly potentiate inhibition of beta-amyloid aggregation. *Chem-biochem* **2007**, *8*, 1857–1864.
- (13) Trudeau, K. M.; Colby, A. H.; Zeng, J.; Las, G.; Feng, J. H.; Grinstaff, M. W.; Shirihai, O. S. Lysosome acidification by photoactivated nanoparticles restores autophagy under lipotoxicity. *J. Cell Biol.* **2016**, *214*, 25–34.
- (14) Boas, U.; Heegaard, P. M. H. Dendrimers in drug research. *Chem. Soc. Rev.* **2004**, *33*, 43–63.
- (15) Wu, L.-P.; Ficker, M.; Christensen, J. B.; Trohopoulos, P. N.; Moghimi, S. M. Dendrimers in Medicine: Therapeutic Concepts and Pharmaceutical Challenges. *Bioconjugate Chem.* **2015**, *26*, 1198–1211.
- (16) Sheard, D. E.; Li, W.; O'Brien-Simpson, N. M.; Separovic, F.; Wade, J. D. Peptide Multimerization as Leads for Therapeutic Development. *Biologics* **2022**, *2*, 15–44.
- (17) Kim, D.; Han, S.; Ji, Y.; Moon, S.; Nam, H.; Lee, J. B. Multimeric RNAs for efficient RNA-based therapeutics and vaccines. *J. Controlled Release* **2022**, *345*, 770–785.
- (18) Fitzpatrick, E. A.; Wang, J.; Strome, S. E. Engineering of Fc Multimers as a Protein Therapy for Autoimmune Disease. *Front. Immunol.* **2020**, *11*, 496.
- (19) Ganta, S.; Deshpande, D.; Korde, A.; Amiji, M. A review of multifunctional nanoemulsion systems to overcome oral and CNS drug delivery barriers. *Mol. Membr. Biol.* **2010**, *27*, 260–273.
- (20) Cunha, A.; Prévot, G.; Mousli, Y.; Barthélémy, P.; Crauste-Manciet, S.; Dehay, B.; Desvergnès, V. Synthesis and Intracellular Uptake of Rhodamine-Nucleolipid Conjugates into a Nanoemulsion Vehicle. *ACS Omega* **2020**, *5*, 5815–5823.
- (21) Jaishy, B.; Abel, E. D. Lipids, lysosomes, autophagy. *J. Lipid Res.* **2016**, *57*, 1619–1635.
- (22) Las, G.; Serada, S. B.; Wikstrom, J. D.; Twig, G.; Shirihai, O. S. Fatty Acids Suppress Autophagic Turnover in β -Cells. *J. Biol. Chem.* **2011**, *286*, 42534–42544.
- (23) Bracci, L.; Falciani, C.; Lelli, B.; Lozzi, L.; Runci, Y.; Pini, A.; De Montis, M.; Tagliamonte, A.; Neri, P. Synthetic peptides in the form of dendrimers become resistant to protease activity. *J. Biol. Chem.* **2003**, *278*, 46590–46595.
- (24) Pardridge, W. M. The blood-brain barrier: bottleneck in brain drug development. *NeuroRx* **2005**, *2*, 3–14.
- (25) Riccardi, C.; Napolitano, F.; Montesarchio, D.; Sampaolo, S.; Melone, M. A. B. Nanoparticle-Guided Brain Drug Delivery: Expanding the Therapeutic Approach to Neurodegenerative Diseases. *Pharmaceutics* **2021**, *13*, 1897.

(26) Nirale, P.; Paul, A.; Yadav, K. S. Nanoemulsions for targeting the neurodegenerative diseases: Alzheimer's, Parkinson's and Prion's. *Life Sci.* **2020**, *245*, 117394.

(27) Harun, S. N.; Amin Nordin, S. A.; Abd Gani, S. S. A.; Shamsuddin, A. F.; Basri, M.; Bin Basri, H. B. Development of nanoemulsion for efficient brain parenteral delivery of cefuroxime: designs, characterizations, and pharmacokinetics. *Int. J. Nanomed.* **2018**, *13*, 2571–2584.

(28) Usenovic, M.; Krainc, D. Lysosomal dysfunction in neurodegeneration: the role of ATP13A2/PARK9. *Autophagy* **2012**, *8*, 987–988.

(29) Dehay, B.; Martinez-Vicente, M.; Caldwell, G. A.; Caldwell, K. A.; Yue, Z.; Cookson, M. R.; Klein, C.; Vila, M.; Bezdard, E. Lysosomal impairment in Parkinson's disease. *Mov. Disord.* **2013**, *28*, 725–732.

(30) Bento, C. F.; Ashkenazi, A.; Jimenez-Sanchez, M.; Rubinsztein, D. C. The Parkinson's disease-associated genes ATP13A2 and SYT11 regulate autophagy via a common pathway. *Nat. Commun.* **2016**, *7*, 11803.

(31) van Veen, S.; Martin, S.; Van den Haute, C.; Benoy, V.; Lyons, J.; Vanhoutte, R.; et al. ATP13A2 deficiency disrupts lysosomal polyamine export. *Nature* **2020**, *578*, 419–424.

(32) Takano, T.; Black, W. J.; Peters, T. J.; de Duve, C. Assay, Kinetics, and Lysosomal Localization of an Acid Cholesteryl Esterase in Rabbit Aortic Smooth Muscle Cells. *J. Biol. Chem.* **1974**, *249*, 6732–6737.

(33) Filograna, R.; Civiero, L.; Ferrari, V.; Codolo, G.; Greggio, E.; Bubacco, L.; et al. Analysis of the Catecholaminergic Phenotype in Human SH-Sy5y and BE(2)-M17 Neuroblastoma Cell Lines upon Differentiation. *PLoS One* **2015**, *10*, No. e0136769.

(34) Dehay, B.; Ramirez, A.; Martinez-Vicente, M.; Perier, C.; Cannon, M.-H.; Doudnikoff, E.; et al. Loss of P-type ATPase ATP13A2/PARK9 Function Induces General Lysosomal Deficiency and Leads to Parkinson Disease Neurodegeneration. *Proc. Natl. Acad. Sci. U.S.A.* **2012**, *109*, 9611–9616.

Supporting Information

Modulating lysosomal pH through innovative multimerized succinic acid-based nucleolipid derivatives

Mathias Brouillard¹, Rémi Kinet², Marie Joyeux¹, Benjamin Dehay^{2*}, Sylvie Crauste-Manciet^{3,4}, and Valérie Desvergnès^{1*}

¹ University of Bordeaux, INSERM U1212, UMR CNRS 5320, Bordeaux, France

² Univ. de Bordeaux, CNRS, IMN, UMR 5293, F-33000 Bordeaux, France

³ MINT UMR INSERM 1066/CNRS 6021, Angers, France

⁴ University Hospital, CHU d'Angers, France

* Correspondence should be addressed to Dr. Benjamin Dehay, Institut des Maladies Neurodégénératives, Université de Bordeaux, CNRS UMR 5293, Centre Broca Nouvelle-Aquitaine, 146 rue Léo Saignat, 33076 Bordeaux CEDEX, France. E-mail: benjamin.dehay@u-bordeaux.fr and Dr. Valérie Desvergnès, Université de Bordeaux, INSERM U1212, UMR CNRS 5320, 146 rue Léo Saignat, 33076 Bordeaux CEDEX, France. E-mail: valerie.desvergnès@u-bordeaux.fr

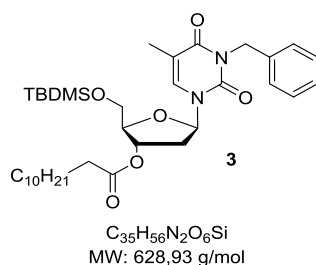
General information.....	2
Synthesis and characterization of compounds 3 , 6 , 9	2
NEs titration curves	5
Cell viability assays.....	6
Characterization of NE- 6 , NE- 7 , NE- 8 loaded with, NL- 6 , 7 and 8	7
¹ H and ¹³ C NMR spectra.....	8

General information

^1H NMR and ^{13}C NMR were recorded at 293 K on a Bruker Avance 300 (^1H : 300 MHz, ^{13}C : 75.46 MHz) spectrometer using residual CHCl_3 as an internal reference (7.26 ppm). The chemical shifts (δ) and coupling constants (J) are expressed in ppm and Hz. The following abbreviations were used to explain the multiplicities: s = singlet, d = doublet, t = triplet and m = multiplet. Fourier transform infrared (FT-IR) spectra were recorded on a PerkinElmer FT spectrometer Spectrum two (UATR two). For electrospray ionization (ESI) high-resolution mass spectrometry (HRMS) analyses, a Waters Micromass ZQ instrument equipped with an electrospray source was used in the positive and/or negative mode. Matrix-assisted laser desorption ionization time-of-flight (MALDI-TOF) mass spectrometric analyses were performed on a PerSeptive Biosystems Voyager-De Pro MALDI mass spectrometer in the linear mode using 3,4-dihydroxybenzoic acid as the matrix. Analytical thin-layer chromatography was performed using silica gel 60 F254 precoated plates (Merck) with visualization by ultraviolet light, potassium permanganate, or sulfuric acid. Flash chromatography was performed on a silica gel (0.043–0.063 mm).

Synthesis and characterization of compounds **4**, **5**, **7**, **8**, **10** and **11** were previously described¹.

Synthesis and characterization of Compound **3**



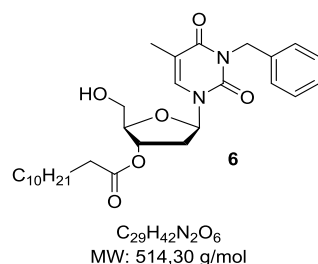
To a solution of compound **2** (1 eq., 1.5 g, 3.36 mmol) into dry DCM (20 mL), were added under argon the lauric acid (1.5 eq., 1.01 g, 5.04 mmol) the EDC.HCl (1.5 eq., 0.96 g, 5.04 mmol) and the DMAP (0.7 eq., 0.52 g, 2.35 mmol). The reaction mixture was stirred at room temperature for 48h, before being quenched with water (20 mL). The aqueous phase was extracted three times with DCM (3 x 30 mL) and the combined organic phases were dried over Na_2SO_4 before being concentrated to dryness under vacuum. The crude product was purified by flash chromatography over silica gel (Pentane/EtOAc: 70/30 to provide compound **3** as a white foam (1.55 g, **73%**).

R_f = 0.9 (Pentane/EtOAc: 70/30); **IR (ATR) ν_{max} (cm^{-1})** 3325, 2965, 2694, 1978, 1738, 1635, 1562, 1492, 1380, 1168, 1066, 994; **^1H -NMR (300 MHz, CDCl_3) δ (ppm)** 7.50 (d, J = 1.2 Hz, 1H), 7.49 - 7.42 (m, 2H), 7.30 - 7.15 (m, 3H), 6.38 (dd, J = 5.4, 9.3 Hz, 1H), 5.27 - 5.19 (m, 1H), 5.15 - 5.03 (m, 2H), 4.04 (d, J = 1.2 Hz,

¹ Brouillard, M., Barthélémy, P., Dehay, B., Crauste-Manciet, S., and Desvergnès, V. (2021) Nucleolipid Acid-Based Nanocarriers Restore Neuronal Lysosomal Acidification Defects. *Front. Chem.* 9:736554.

1H), 3.94 - 3.82 (m, 2H), 2.38 (dd, $J = 5.4, 13.5$ Hz, 1H), 2.29 (appearing t, $J = 7.2, 7.5$ Hz, 2H), 2.15 - 2.01 (m, 2H), 1.92 (d, $J = 0.6$ Hz, 3H), 1.67 - 1.53 (m, 2H), 1.36 - 1.18 (m, 18H), 0.96 - 0.79 (m, 12H), 0.11 (s, 3H), 0.11 (s, 3H); $^{13}\text{C-NMR}$ (75.5 MHz, CDCl_3) δ (ppm) 173.1, 163.1, 150.8, 136.9, 133.0, 129.1, 128.1, 127.3, 110.2, 85.3, 85.3, 75.0, 63.5, 53.3, 44.3, 38.0, 34.0, 31.8, 30.6, 29.4, 29.3, 29.2, 29.1, 29.0, 25.8, 24.6, 22.5, 18.1, 14.0, 13.1, -5.6, -5.7; **HRMS (ESI)**: Calcd. for $\text{C}_{35}\text{H}_{56}\text{N}_2\text{O}_6\text{Si}$ $[\text{M}+\text{H}]^+$ 629.39076, found 629.39866.

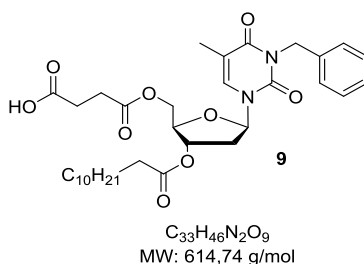
Synthesis and characterization of Compound 6



To a solution of compound 3 (1 eq., 1.55 g, 2.46 mmol) into dry THF (28 mL), was added at 0°C, under argon the TBAF (1 eq., 0.710 mL, 2.46 mmol). The reaction mixture was stirred at 0°C for 3h, before being quenched with water (30 mL). The aqueous phase was extracted three times with DCM (3 x 30 mL) and the combined organic phases were dried over Na_2SO_4 before being concentrated to dryness under vacuum. The crude product was purified by flash chromatography over silica gel (Pentane/EtOAc: 70/30) to provide compound 6 as a white foam (1.27 g, 90%).

$R_f = 0.3$ (Pentane/EtOAc: 70/30); **IR (ATR) ν_{max} (cm^{-1})** 3361, 2926, 2859, 1931, 1649, 1457, 1359, 1170, 1104, 704; $^1\text{H-NMR}$ (300 MHz, CDCl_3) δ (ppm) 7.68 (d, $J = 0.6$ Hz, 1H), 7.45 - 7.38 (m, 2H), 7.27 - 7.14 (m, 3H), 6.32 (appearing t, $J = 8.1, 6.3$ Hz, 1H), 5.34 - 5.28 (m, 1H), 5.11 - 5.05 (m, 2H), 4.05 - 4.00 (m, 1H), 3.85 - 3.74 (m, 2H), 2.36 - 2.24 (m, 4H), 1.85 (brs, 3H), 1.66 - 1.52 (m, 2H), 1.35 - 1.17 (m, 18H), 0.91 - 0.80 (m, 3H); $^{13}\text{C-NMR}$ (75.5 MHz, CDCl_3) δ (ppm) 173.3, 163.4, 150.8, 136.5, 134.5, 128.7, 128.2, 127.4, 110.1, 86.0, 85.1, 74.7, 62.2, 44.3, 37.5, 34.0, 31.7, 29.4, 29.3, 29.1, 29.1, 28.9, 24.6, 22.5, 14.0, 13.1; **HRMS (ESI)**: Calcd. for $\text{C}_{29}\text{H}_{42}\text{N}_2\text{O}_6$ $[\text{M}+\text{H}]^+$ 515.30429, found 515.31170.

Synthesis and characterization of Compound 9



To a suspension of nucleolipid 6 (1eq., 500 mg, 0.88 mmol) into dry toluene (10 mL), were added under argon succinic anhydride (1eq., 88 mg, 0.88 mmol) and DMAP (0.1 eq., 10 mg, 0.088 mmol). The reaction mixture

was heated at 140°C and stirred for 2 hours before being concentrated under vacuum. The crude product was purified by flash chromatography over silica gel (Toluene/EtOAc: 80/20) to provide compound **9** as a colorless gum (270 mg, **50%**).

R_f = 0.1 (Toluene/Acetone: 80/20); **IR (ATR) v_{max} (cm⁻¹)** 2927, 2859, 2254, 1905, 1831, 1723, 1647, 1563, 1454, 1406, 1357, 1255, 1159, 1101, 1005, 910, 828, 728, 628, 534; **¹H-NMR (300 MHz, CDCl₃) δ (ppm)** 8.30 (brs, 1H), 7.50 - 7.42 (m, 2H), 7.34 - 7.19 (m, 4H), 6.33 (dd, *J* = 5.4, 8.4 Hz, 1H), 5.23 - 5.14 (m, 1H), 5.14 - 5.05 (m, 2H), 4.44 (dd, *J* = 4.2, 12.3 Hz, 1H), 4.33 (dd, *J* = 3.0, 12.0 Hz, 1H), 4.24 - 4.17 (m, 1H), 2.72 - 2.58 (m, 4H), 2.44 (dd, *J* = 4.8, 13.5 Hz, 1H), 2.32 (*appearing t*, *J* = 7.2, 7.8 Hz, 2H), 2.21 - 2.08 (m, 1H), 1.94 (brs, 3H), 1.68 - 1.54 (m, 2H), 1.38 - 1.17 (m, 18H), 0.93 - 0.81 (m, 3H); **¹³C-NMR (75.5 MHz, CDCl₃) δ (ppm)** 176.8, 173.4, 171.8, 163.4, 150.9, 136.7, 133.0, 129.1, 129.1, 128.4, 128.4, 127.7, 110.8, 85.5, 82.2, 74.0, 64.1, 44.6, 37.5, 34.1, 31.9, 29.6, 29.4, 29.3, 29.2, 29.1, 28.7, 28.6, 24.8, 22.7, 14.1, 13.4; **HRMS (ESI):** Calcd. for C₃₃H₄₃N₂O₉ [M+H]⁺ 615.32033, found 615.32846.

NEs titration curves

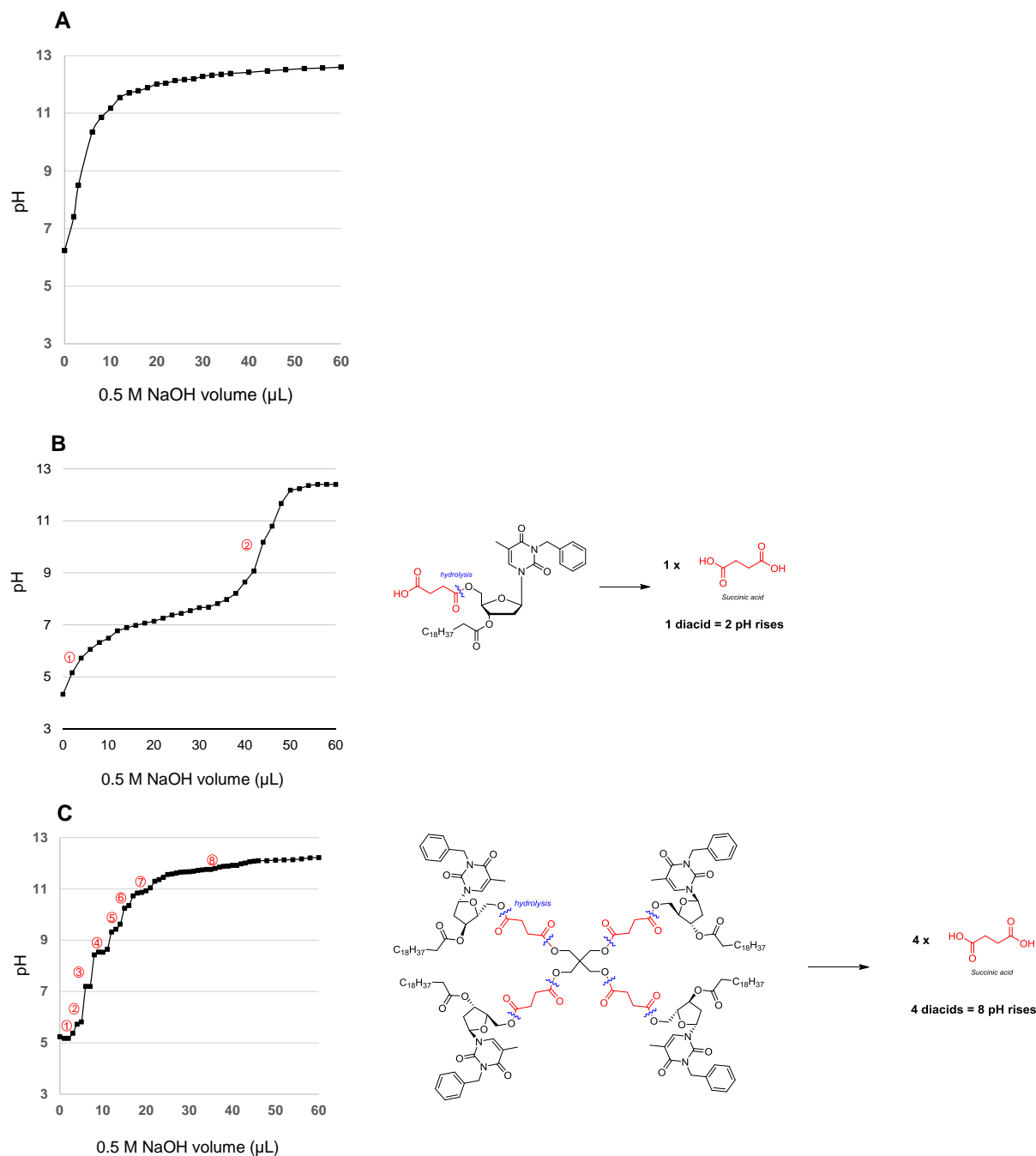


Figure S1. Acid-base titration curves for a control unloaded NE-0 (A), monomer 11 loaded NE-11 (B), and multimer 14 loaded NE-14 (C). The NEs were loaded with 1% (w/w) arachidate NLs 11 and 14, respectively.

Experimental protocol: Acid-base titration curves were performed on 1 mL of NE-11, and NE-14, respectively loaded with 1% (w/w) of monomer 11 and tetramer 14. NaOH (0.5 M) was gradually added to the emulsions under the control of a pH meter. pH was measured after NE homogenization by magnetic stirring. An unloaded

NE-0 was used as control (A). Graph B reports the NE-11 release profile, consistent with a weak diacid titration with 2 visible pH rises. This control test allowed us to validate the feasibility and relevance of titration in a NE.

Cell viability assays

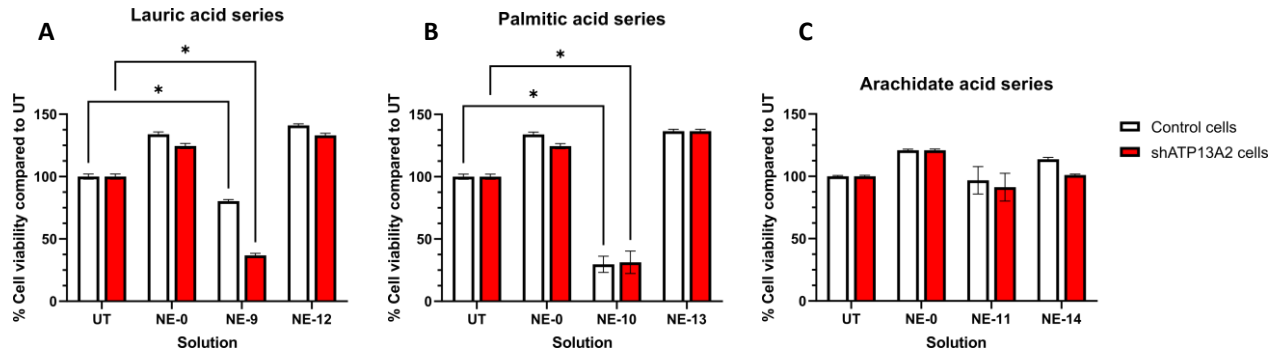


Figure S2. Comparative cell viability in control and ATP13A2-depleted (sh403-1) M17 cells, in the absence (UT) or presence of NE for each fatty chain length 48 hours after treatment. *p < 0.05 compared with untreated cells. A. NE-0, NE-9 and NE-12. B. NE-0, NE-10 and NE-13. C. NE-0, NE-11 and NE-14.

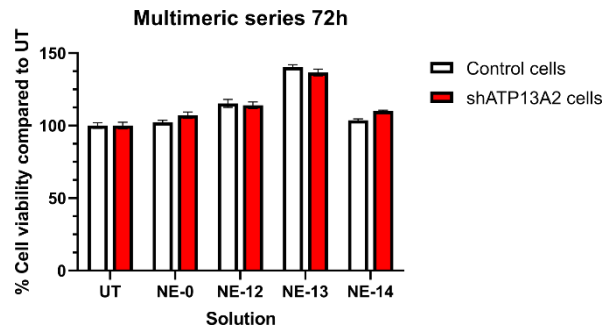


Figure S3. Comparative cell viability in control and ATP13A2-depleted (sh403-1) M17 cells, in the absence (UT) or presence of multimers-loaded NE for each fatty chain length 72 hours after treatment. *p < 0.05 compared with untreated cells.

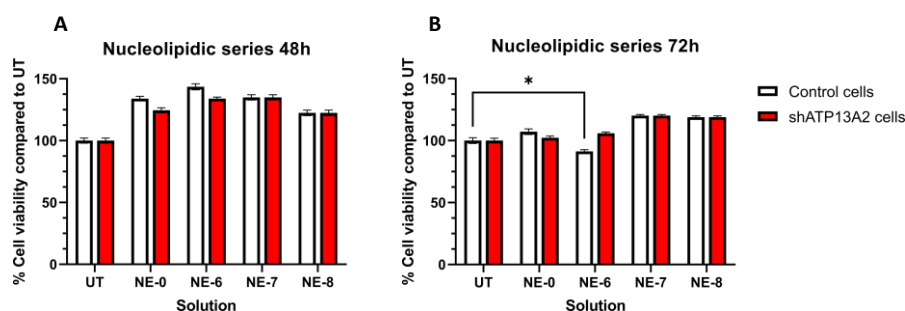


Figure S4. Comparative cell viability in control (shScr-1) and ATP13A2-depleted (sh403-1) M17 cells, in the absence (UT) or presence of 5'-OH NL loaded NE for each fatty chain length 48 hours (A) and 72 hours (B) after cells treatment.

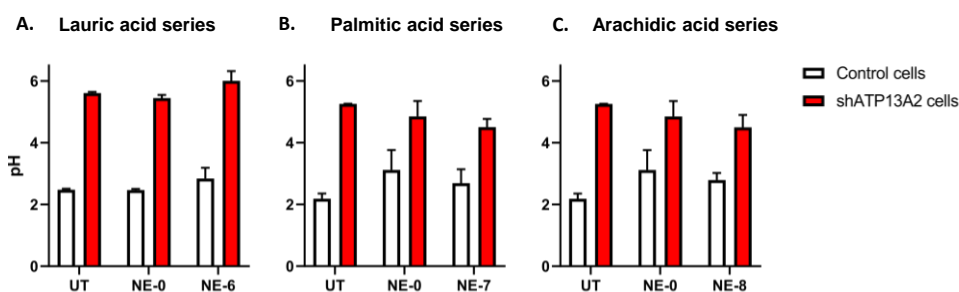


Figure S5. Lysosomal pH *in vitro* in control and ATP13A2-depleted (sh403-1) M17 cells, in the absence (UT) or presence of NE-0 and non-acidic NL-based NE NE-6, NE-7 and NE-8, 24 hours after cells treatment.

Characterization of NE-6, NE-7, NE-8 loaded with, NL-6, 7 and 8 (OH free at 5' position, 3% w/w) respectively.

	NE-0	NE-6	NE-7	NE-8
Droplets mean diameter (nm)	170.4 ± 3.2	195.3 ± 3.2	179.3 ± 3.4	171.9 ± 1.7
Polydispersity index	0.143	0.078	0.099	0.112
Zeta potential (mv)	- 33.6 ± 0.2	- 33.3 ± 0.1	- 30.2 ± 0.4	- 33.9 ± 1.2

Table S1. Physico-chemical characteristics of NLs NEs.

7.507
7.503
7.487
7.421
7.303
7.145

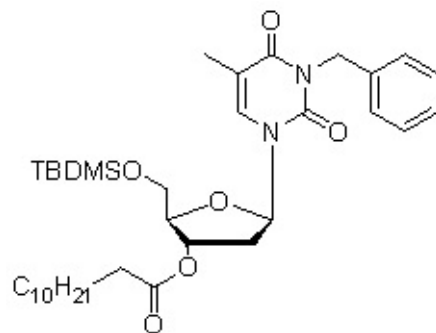
6.402
6.384
6.371
6.354

5.267
5.194
5.147
5.028

4.040
4.036
3.943
3.824

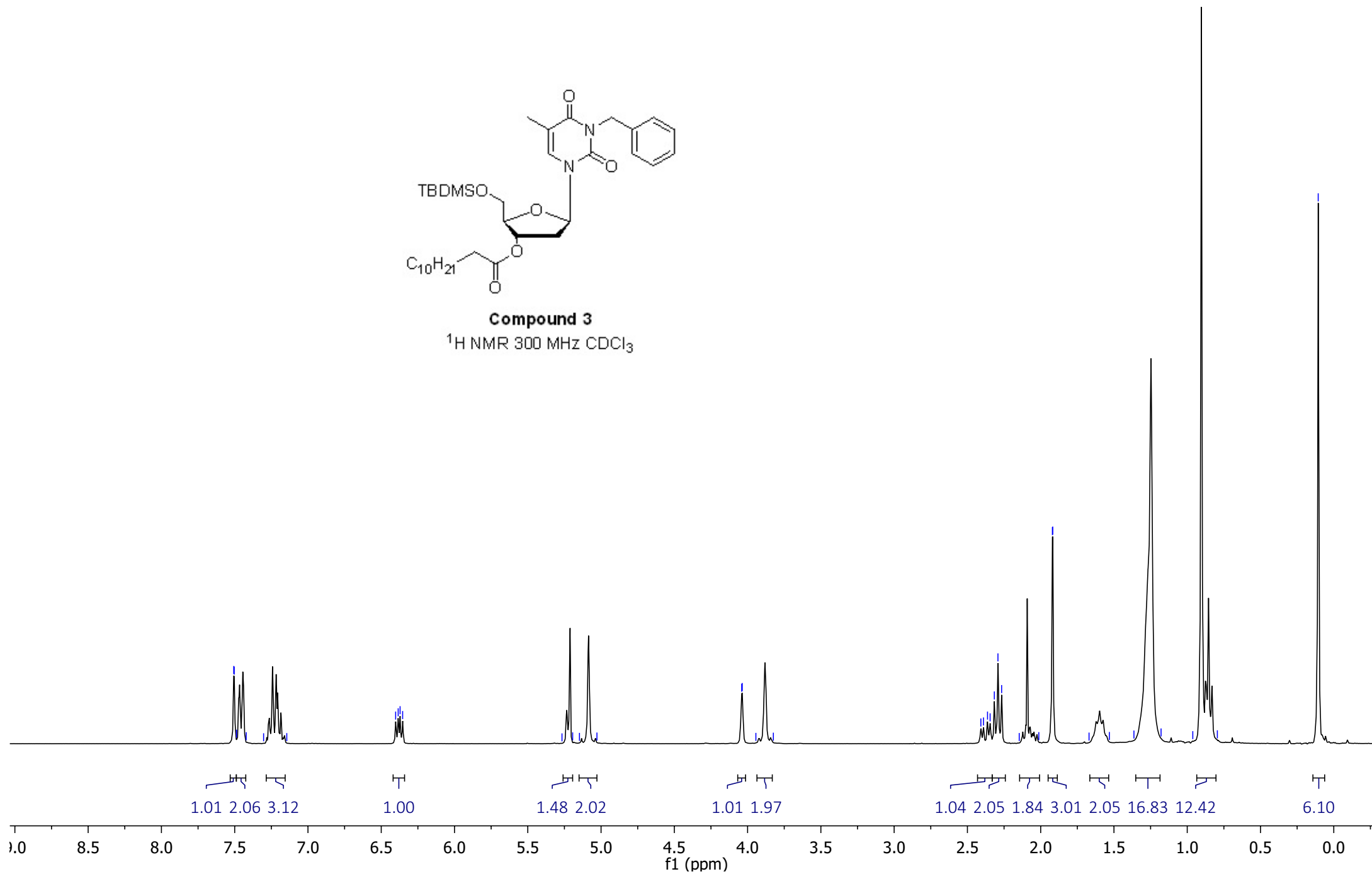
2.408
2.390
2.363
2.345
2.316
2.292
2.267
2.146
2.013
1.920
1.918
1.670
1.551
1.364
1.179
0.962
0.794

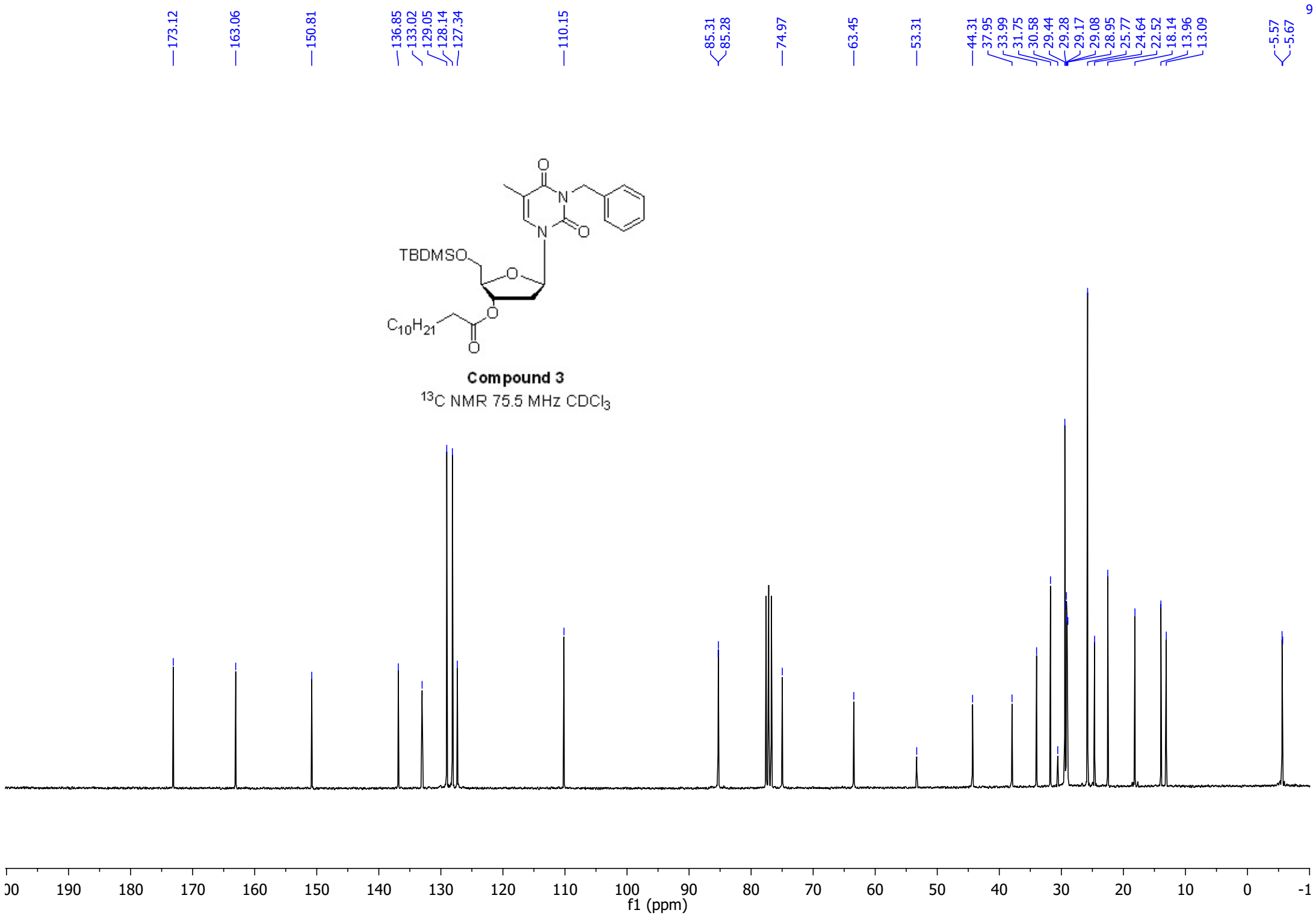
0.106

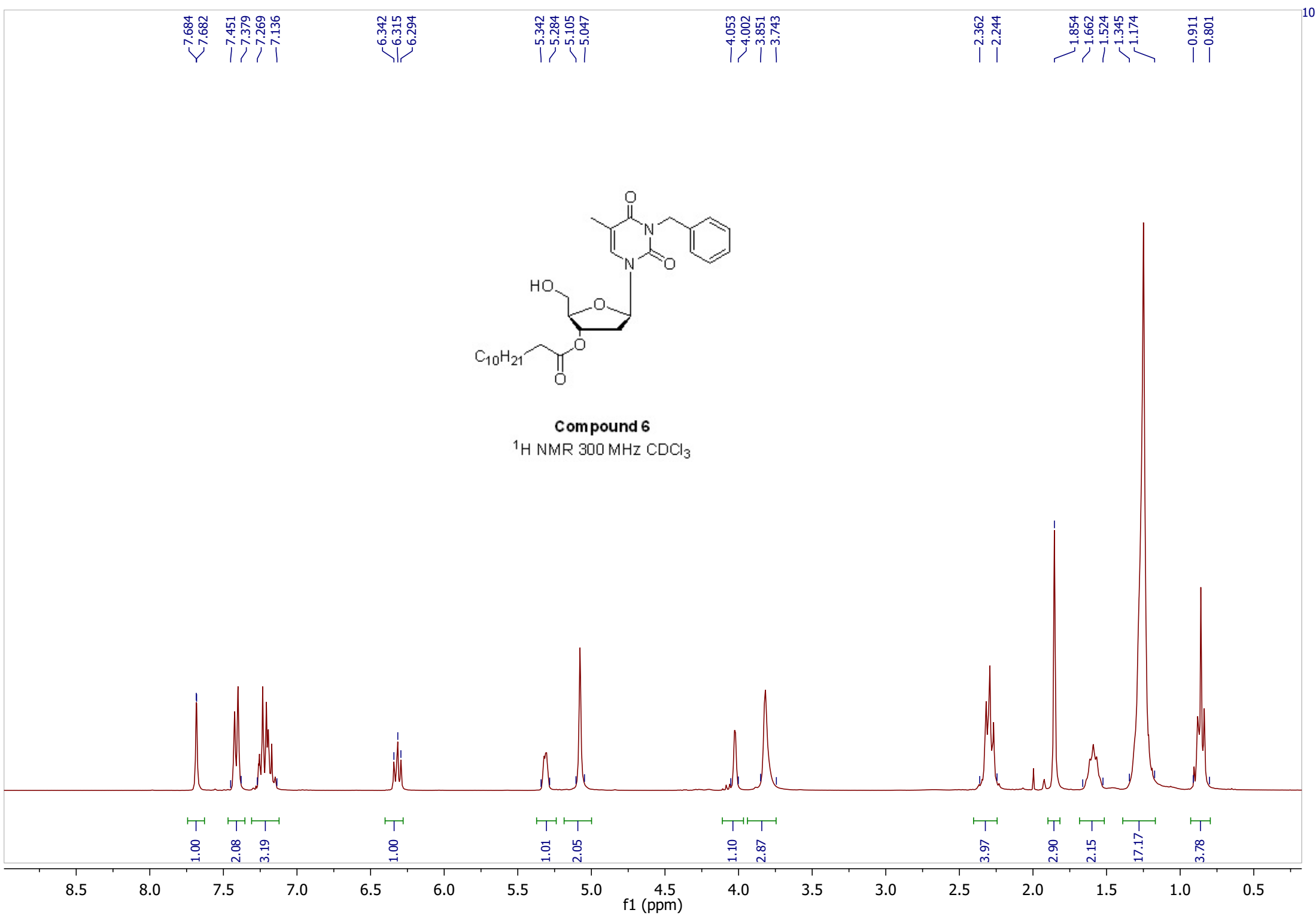


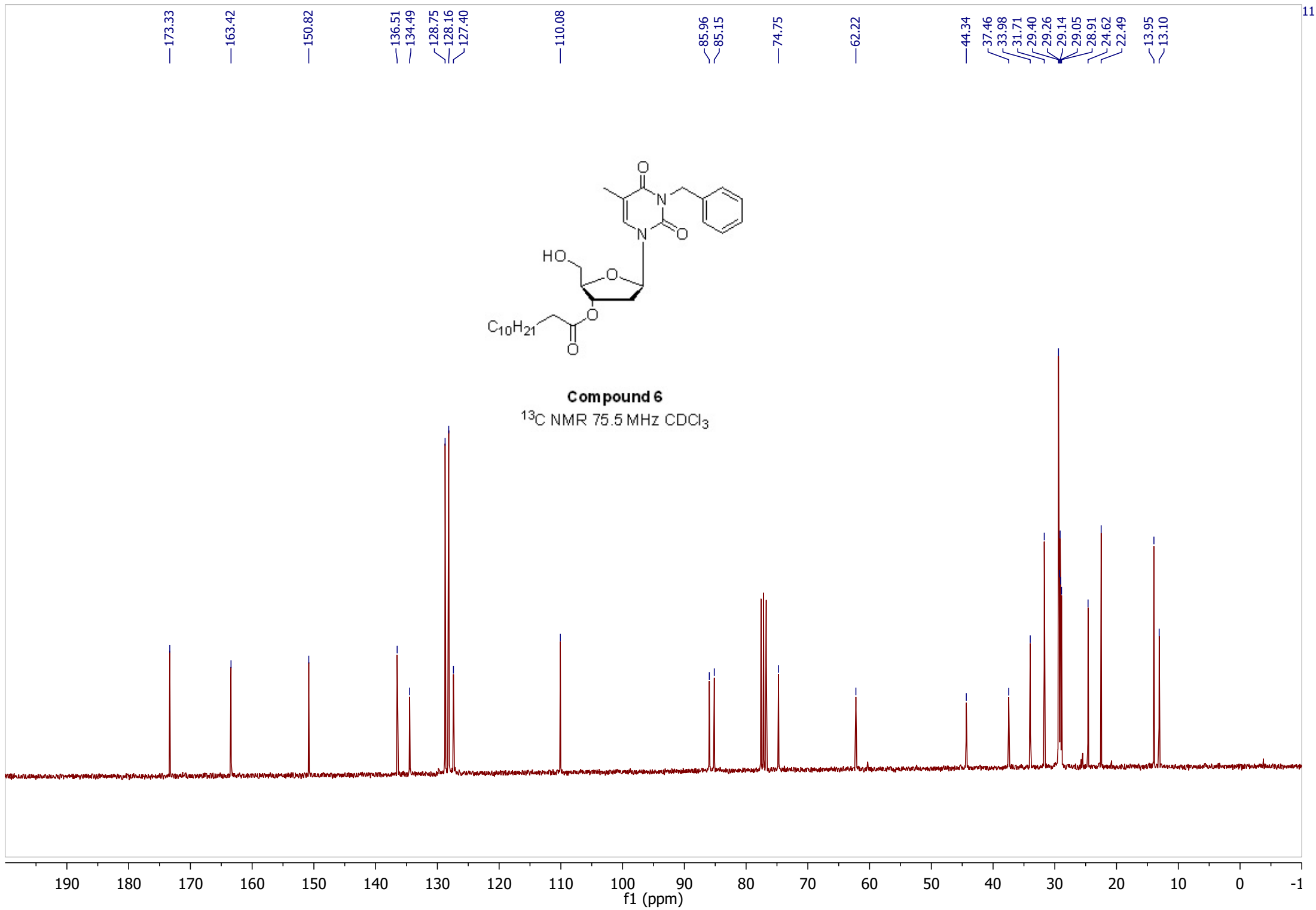
Compound 3

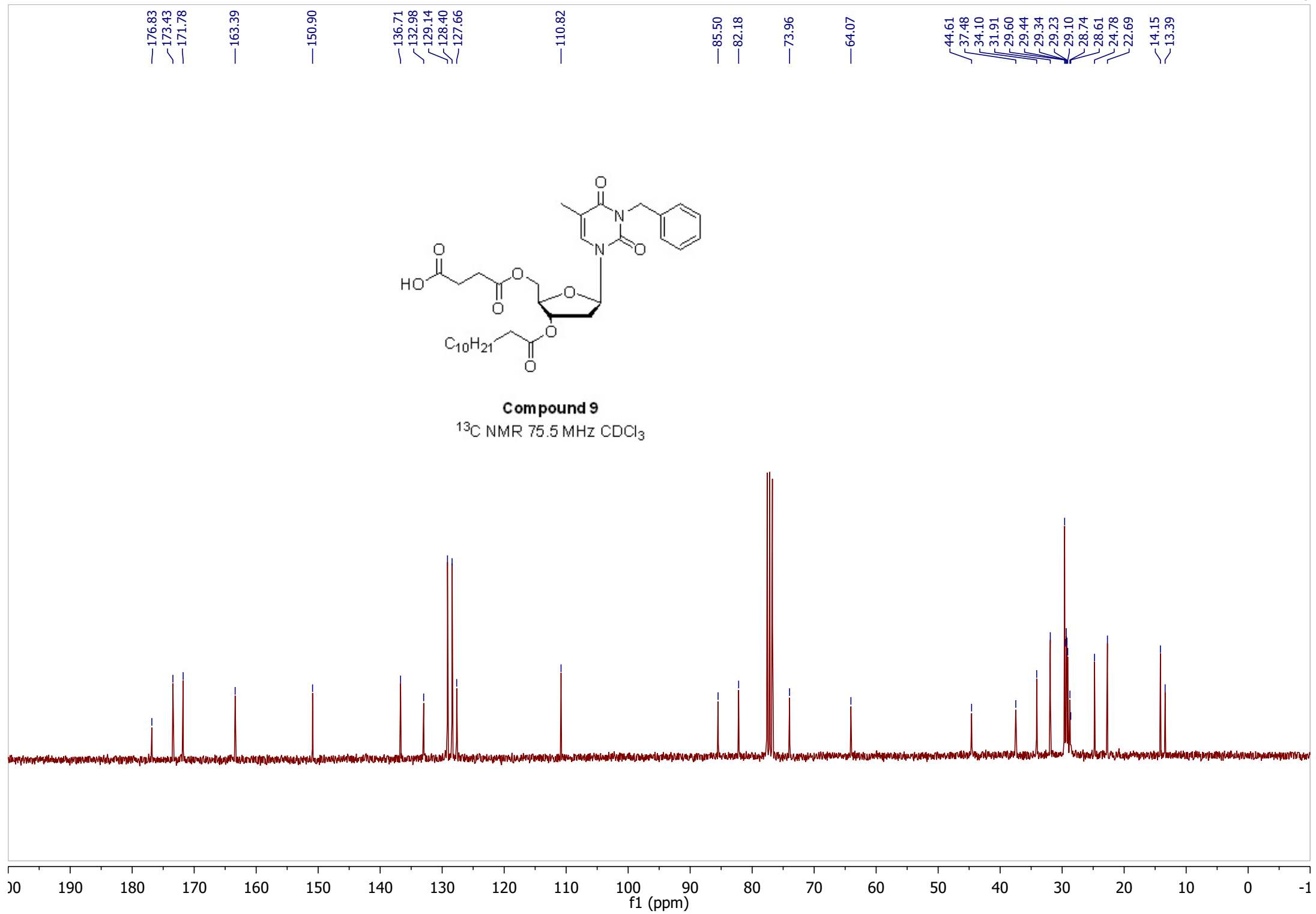
¹H NMR 300 MHz CDCl₃

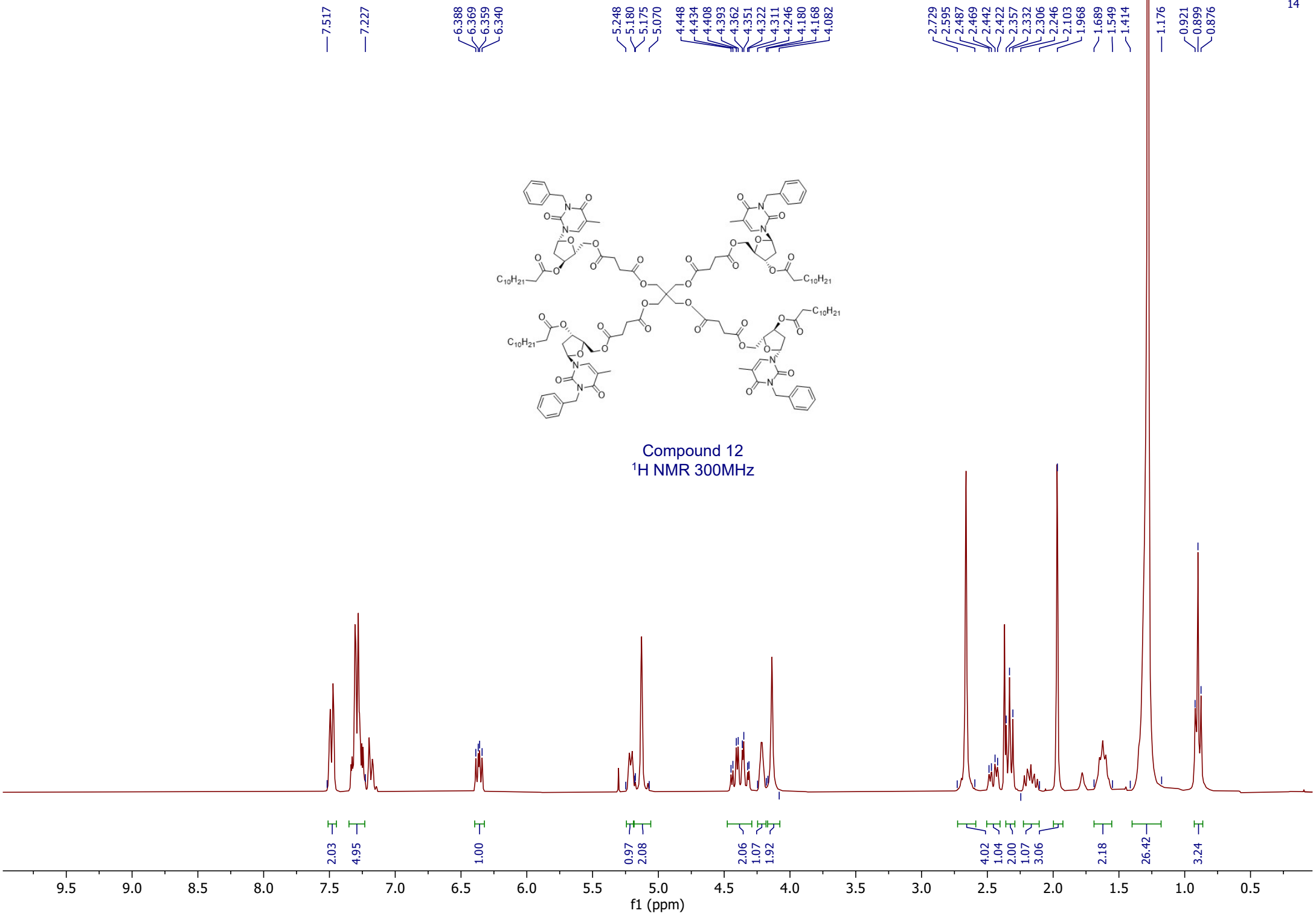


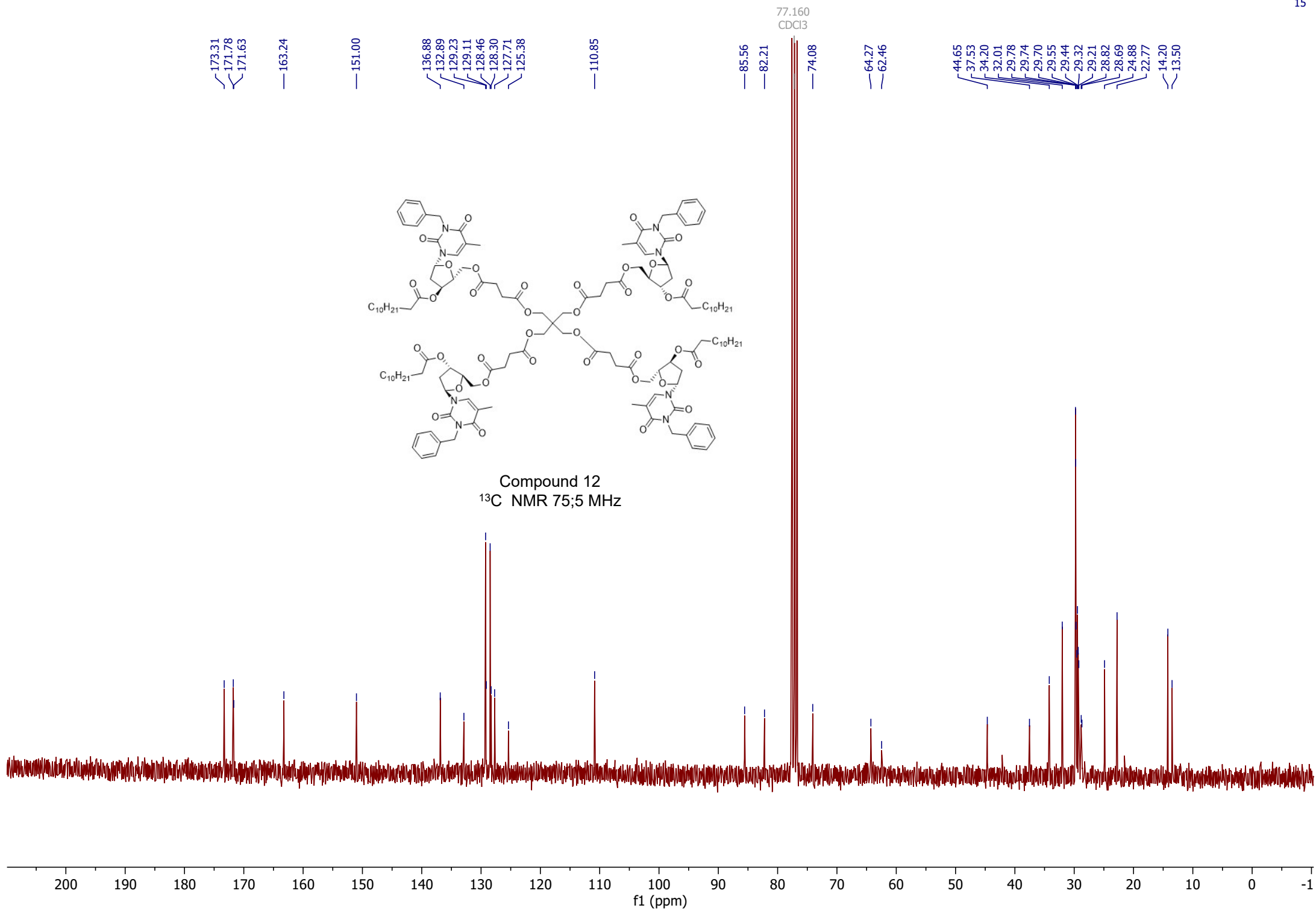


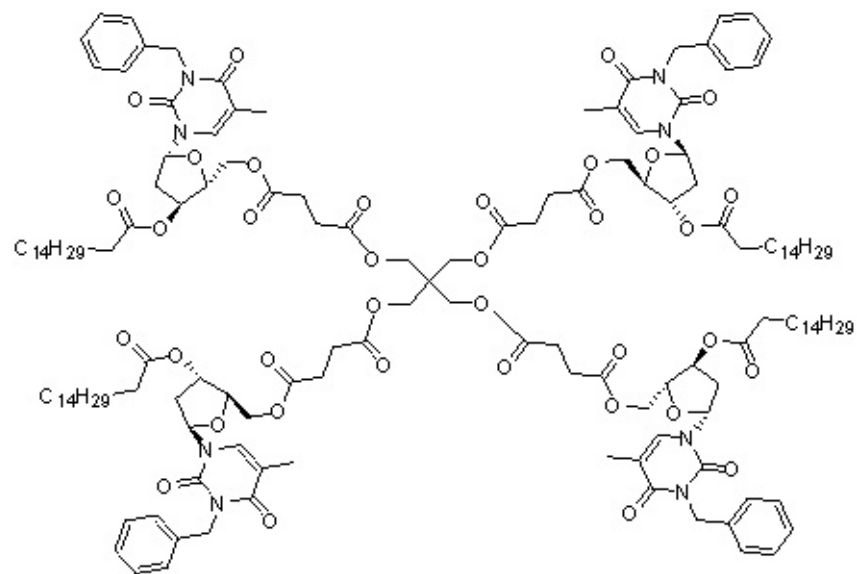




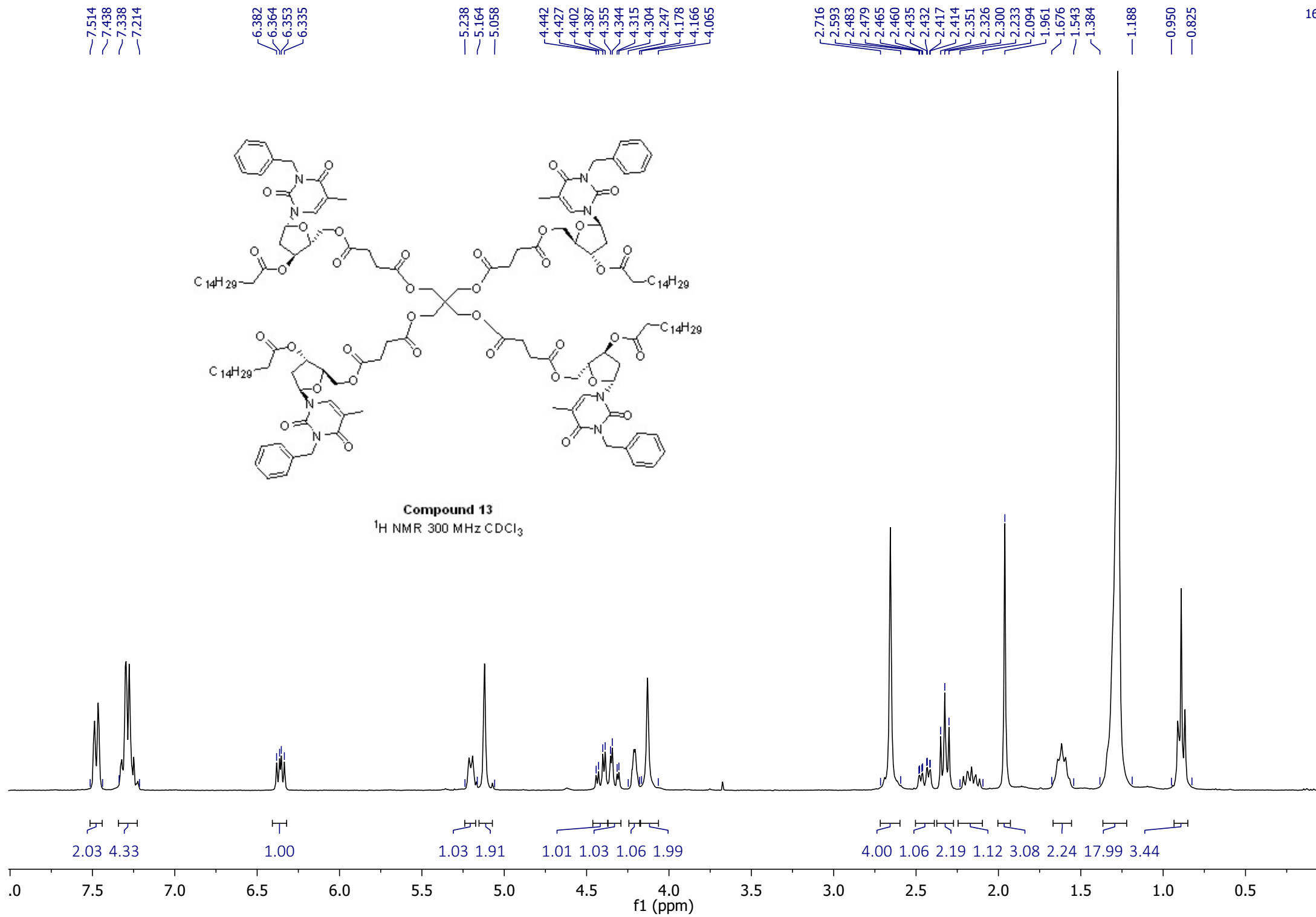


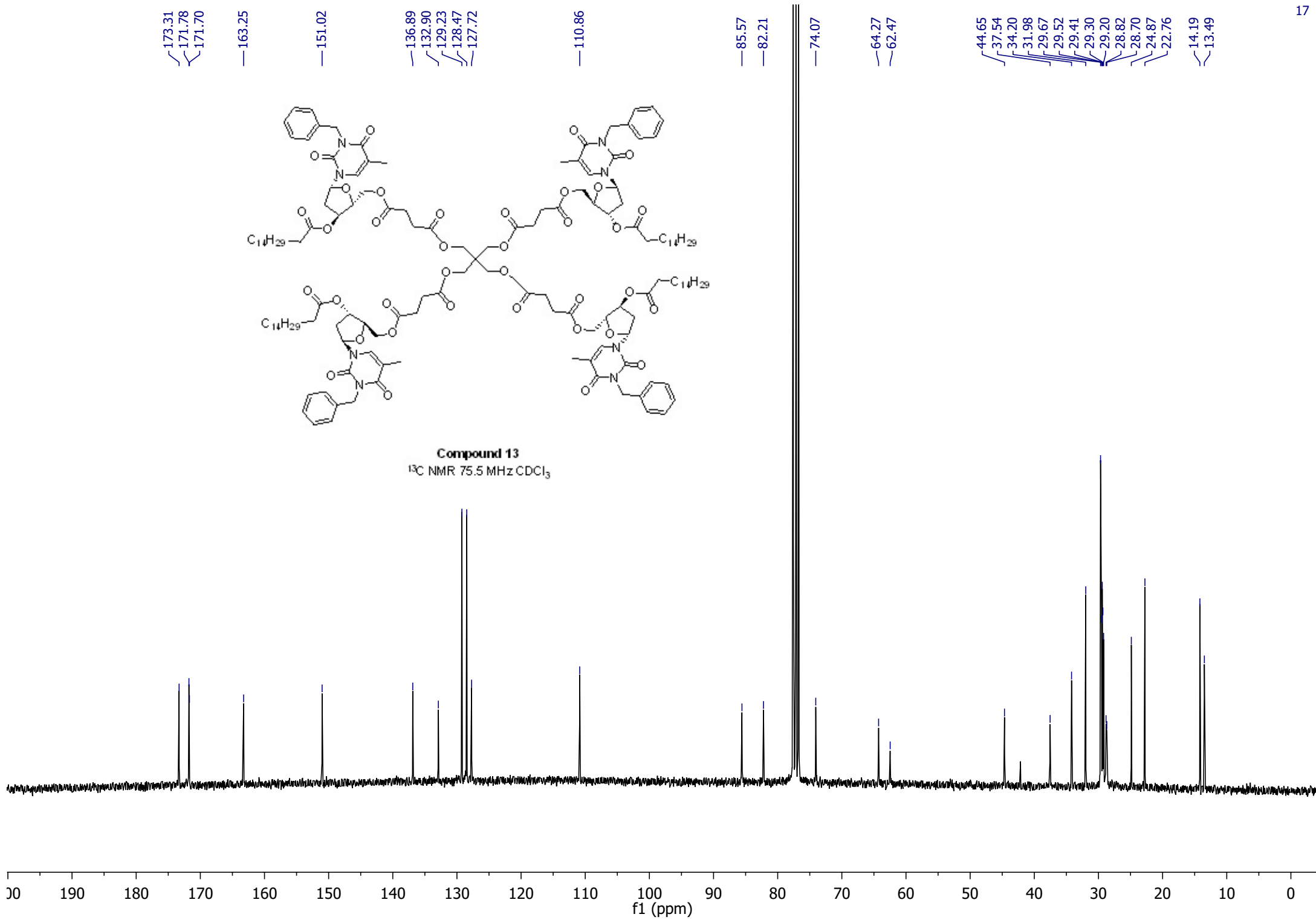






Compound 13
¹H NMR 300 MHz CDCl₃





7.498
7.415
7.335
7.198

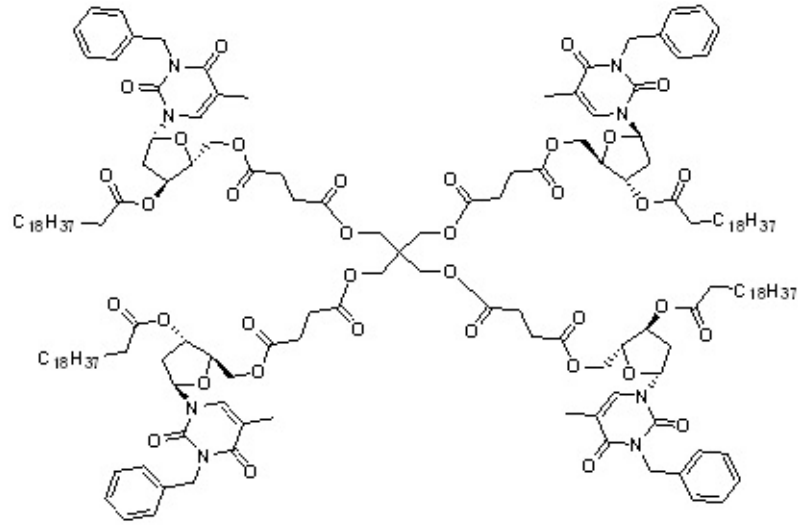
6.363
6.345
6.335
6.316

5.224
5.143
5.043

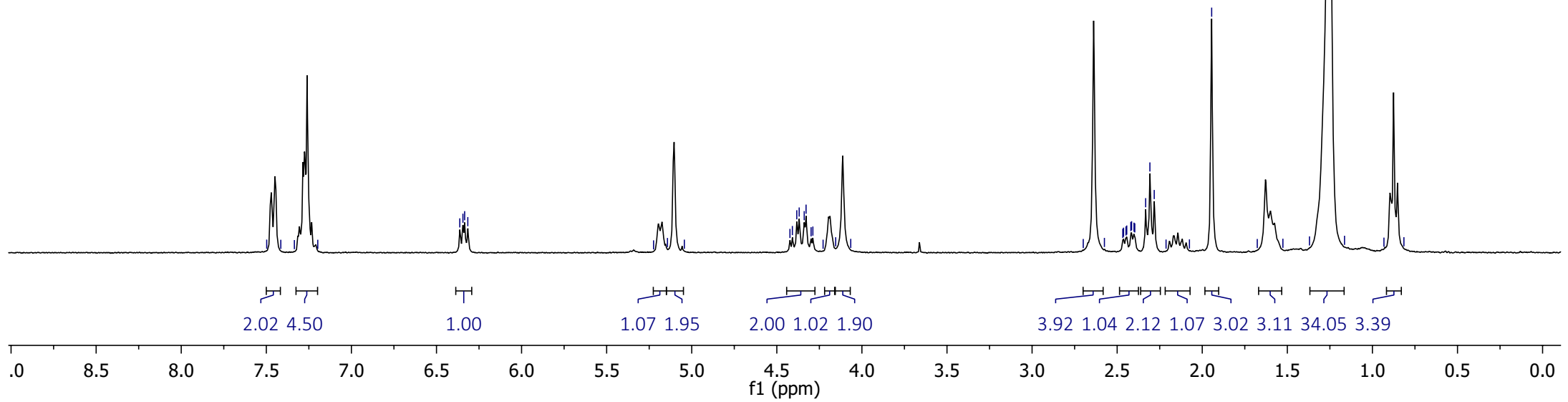
4.423
4.409
4.383
4.369
4.339
4.328
4.299
4.288
4.228
4.154
4.066

2.699
2.575
2.467
2.462
2.448
2.444
2.420
2.415
2.401
2.396
2.333
2.308
2.282
2.213
2.075
1.945
1.677
1.526
1.370
1.164

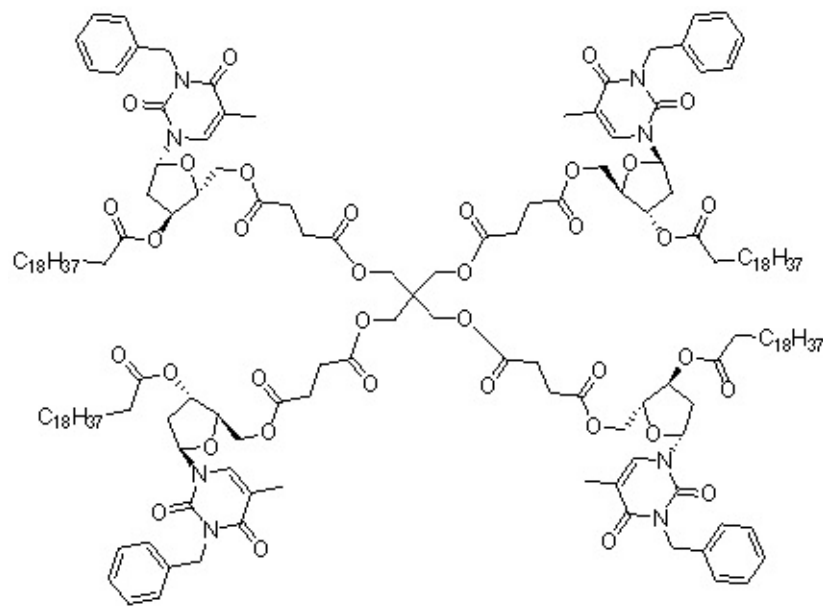
0.932
0.815



Compound 14
¹H NMR 300 MHz CDCl₃



173.35
171.81
171.73
163.28
151.05
136.91
132.91
129.27
128.50
127.75
110.89
85.59
82.24
74.11
64.31
62.50
44.68
37.57
34.23
32.04
29.82
29.78
29.74
29.59
29.47
29.36
29.25
28.84
28.71
24.91
22.80
14.23
13.53



Compound 14

¹³C NMR 75.5 MHz CDCl₃

